

Tesi di dottorato in Ingegneria Biomedica, di Giuseppe Cavallo,
discussa presso l'Università Campus Bio-Medico di Roma in data 08/02/2008.
La disseminazione e la riproduzione di questo documento sono consentite per scopi di didattica e ricerca,
a condizione che ne venga citata la fonte.



Università Campus Bio-Medico di Roma
School of Engineering

PhD Course in Biomedical Engineering
(XX - 2004/2007)

Mechatronic Technologies for Behavioural Analysis

Giuseppe Cavallo

A handwritten signature in black ink, reading 'Giuseppe Cavallo'. The signature is written in a cursive, flowing style.

Tesi di dottorato in Ingegneria Biomedica, di Giuseppe Cavallo,
discussa presso l'Università Campus Bio-Medico di Roma in data 08/02/2008.
La disseminazione e la riproduzione di questo documento sono consentite per scopi di didattica e ricerca,
a condizione che ne venga citata la fonte.

Giuseppe Cavallo

Tesi di dottorato in Ingegneria Biomedica, di Giuseppe Cavallo,
discussa presso l'Università Campus Bio-Medico di Roma in data 08/02/2008.
La disseminazione e la riproduzione di questo documento sono consentite per scopi di didattica e ricerca,
a condizione che ne venga citata la fonte.

Mechatronic Technologies for Behavioural Analysis

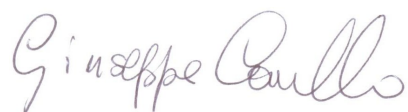
A thesis presented by
Giuseppe Cavallo
in partial fulfillment of the requirements for the degree of
Doctor of Philosophy
in Biomedical Engineering
Università Campus Bio-Medico di Roma
School of Engineering

Coordinator
Prof. Saverio Cristina

Supervisor
Prof. Eugenio Guglielmelli

Co-Supervisors
Prof. Flavio Keller
Dr. Domenico Campolo

January 2008



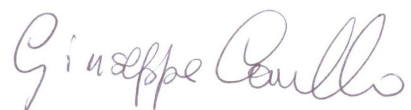
Tesi di dottorato in Ingegneria Biomedica, di Giuseppe Cavallo,
discussa presso l'Università Campus Bio-Medico di Roma in data 08/02/2008.
La disseminazione e la riproduzione di questo documento sono consentite per scopi di didattica e ricerca,
a condizione che ne venga citata la fonte.

Alla mia nonna

Giuseppe Cavallo

Contents

Contents	v
List of Tables	vii
List of Figures	viii
1 Introduction	1
1.1 Behavioural Analysis	1
1.1.1 Behavioural Phenotyping	2
1.1.2 The animal models	4
1.2 The mechatronic paradigm	5
1.3 The proposed approach	7
2 A tremor detecting platform	11
2.1 Introduction	11
2.2 Rationale	12
2.3 The force platform	13
2.4 Functional and technical specifications	14
2.5 Design of the platform	16
2.5.1 Primary transducers	17
2.5.2 Secondary transducer	21
2.6 Experimental setup and calibration	23
2.6.1 Static calibration	25
2.6.2 The dynamic calibration	25
2.7 Preliminary tests and data analysis	27
2.8 Conclusion and future developments	31
3 The catching platform	33

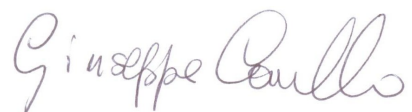


3.1	Rationale	34
3.2	The catching platform	34
3.2.1	Design of the catching apparatus	36
3.2.2	The sensory system	37
3.3	Applications of the catching platform	39
3.3.1	Motion analysis and experimental protocol	40
3.4	Experimental trials and preliminary results	41
3.5	Conclusions	45
4	Neurodevelopmental Engineering	47
4.1	Introduction	47
4.2	Autism as neurodevelopmental disorder	48
4.3	Tools for early diagnosis	49
4.4	The calibration issue	50
4.5	The proposed solution: in-field calibration	51
4.5.1	Magneto/Inertial orientation tracking	51
4.5.2	The calibration procedure	53
4.5.3	Experimental setup and results	56
4.6	Conclusions	57
5	Isometric measurements in post-stroke patients	59
5.1	Rationale	59
5.2	The ALLADIN platform	61
5.2.1	The data collected	63
5.3	The approach and the proposed solution	63
5.3.1	Features definition	65
5.3.2	Onset detection	69
5.4	Comparative evaluation and results	72
5.4.1	The ALLADIN pre-processing tool	74
5.4.2	The ALLADIN filtering module (AFM)	75
5.4.3	The ALLADIN previsualization module (AVM)	75
5.4.4	The ALLADIN feature extraction module (AFEM)	76
5.4.5	APT testing	77
5.5	Conclusion	78
	Conclusions	79
	Bibliography	87



List of Tables

5.1	Position of ADD F/T sensors on patient's body	62
5.2	Activity of Daily Living tasks to be performed by the patient . . .	63
5.3	Results of the comparative study of different onset of movement detection methods. Mean value, standard deviation, variance and median are related to the error distribution. The mean absolute value is the mean of the error absolute value distribution.	73



List of Figures

1.1	A phenotypic map (yellow) can be generated to correspond to any genomic map (green). Some genes, such as gene1 (g1), have only one corresponding phenotype (p1), whereas most genes have many corresponding phenotypes. Phenotypes can be coded for by more than one gene, as shown by p2, which is affected by g2 and g5. . .	3
1.2	The integrated approach of multidisciplinary features brings to Mechatronics, which integrates many engineering fields to the development of innovative products in several commercial areas.	7
1.3	The possible application of behavioural analysis: the blocks represent the single research activities preformed during the PhD and reported in this thesis	8
2.1	The mechanical structure of the sensor consisting of two tiles (central holes simply reduce mass) kept parallel by four long and thin pillars (a). Each pillar has both ends constrained to be perpendicular to the tiles. Long and thin pillars are used to provide enough compliance in the transversal direction while being extremely stiff in the axial direction, therefore only in-plane forces cause detectable deformation (b). By clamping the bottom tile to the ground, the top one is constrained to move parallelly to the ground, i.e. the structure is practically not deformed by weight forces and torques.	18



2.2	The self-aligned assembly procedure. Four needles are inserted in the small through holes of the tile and placed in the upright position (a). A centering cylinder is placed through the central hole of the tile (b). Spacing discs are then piled up (c) as the cylinder keeps everything up and steady. When a given number of discs is piled up, the second tile is also inserted (d). After each end of the needles has been glued to the tiles, first the cylinder is removed, then the discs are let slide sideways and then, after cutting off protruding parts of the needles, the structure (e) is finally assembled.	19
2.3	Functional schema (a) and picture (b) of the IR optical proximity sensor	21
2.4	The optical retro-reflective IR proximity sensor calibration curve is highly non-linear, but it can be linearized under the hypothesis of small displacement (i.e. $\pm 100\mu m$)	22
2.5	Experimental setup	23
2.6	Calibration setup	24
2.7	Time plot (top) and frequency plot (bottom) of the normalized impulse response of the mechanical structure.	24
2.8	Results of the dynamic calibration. (a) V_{opt} vs Δx derived from the double integration of the acceleration signal. (b) The two calibration curves obtained from static and dynamic procedures. The two lines can be considered overlapped	27
2.9	Spectrograms for Wildtype (top) and Reeler (bottom) tests. The colored peaks give information on the intensity of the respective frequency component for each time interval	28
2.10	Plots for Wildtype (top) and Reeler (bottom) tests. The first and the third plot show the time analysis of particularly interesting time intervals while the second and the fourth plot show the corresponding Fourier analysis highlighting the harmonic content of the signals	29
2.11	A spectrogram related with snapshots taken from the camera. This analysis reveals those very points when the mouse steps on the tile and where it is headed	30
3.1	Design and description of the catching platform	35
3.2	(a) The moving handle with the JR3 load cell beneath. (b) The magneto-inertial sensor (Xsense)	38
3.3	Schema and picture of the experimental setup and the reference frame	41



3.4	Distribution - average on all subjects - of desynchronization (ERD) and synchronization (ERS) in different bands in static catching and dynamic catching. The color blue represents the intensity of the desynchronization, while the red one represents synchronization.	42
3.5	From left to right, acceleration detected by the magneto-inertial sensor and velocity and position extracted from acceleration. In particular the y-component is shown	43
3.6	Reconstruction of the trajectory followed by subject's wrist (top view)	44
3.7	The left plot shows the first 20 tracks (top view) extracted from subject's wrist acceleration signal, the right plot shows the other 20. The starting point was fixed at the axis origin. Trajectories endpoints are moves towards the rest position of the handle as the subject learns the task	45
4.1	Fixed and moving coordinate frames, respectively $\{\mathbf{x}^0, \mathbf{y}^0, \mathbf{z}^0\}$ and $\{\mathbf{x}^1, \mathbf{y}^1, \mathbf{z}^1\}$	52
4.2	Distance of a point P from an ellipse: although BP represents the true geometrical distance, AP is used instead as an analytically convenient approximation.	55
4.3	Measurement sequence: 3-axis sensor's amplified read-outs	56
4.4	<i>Left</i> : "cloud" of measurements, i.e. the trajectory of measurement sequences in 3D space. <i>Right</i> : best fitting ellipsoid (thin lines) superimposed with cloud of measurements (thick lines).	58
5.1	A. The ADD platform installed at Campus Bio-Medico University in Rome: 8 force/torque sensors distributed in 8 body districts allow isometric measurements on Activity of Day Living tasks in post-stroke patients. B. A detail of the orthosis for the assessment of manipulation tasks.	62
5.2	Recovery space paradigm: the stroke patient is represented by a feature vector that ideally evolves over time from his initial state to normality (N).	64
5.3	Application of the ks-density based technique on a sample force measurement	72
5.4	Overall architecture of the APT - Alladin Pre-processing Tool	75
5.5	Testing signals for the force components	77



Chapter 1

Introduction

This work presents the author's research activity during his PhD. The main attention was focused on Behavioural Analysis, a medical discipline aiming at the study of external expressions of a living being to go back to causes generating them. The study of behaviour classically grounds on subjective researcher's observations performed by the assistance of low technological devices (i.e. videotapes). In this dissertation new solutions will be proposed addressing to behavioural analysis targets by the use of mechatronic technologies and approaches.

1.1 Behavioural Analysis

Behavioural analysis is a research discipline whose aim is to characterize and quantify a typical feature belonging to the living beings that has been widely studied in medical and biological literature: behaviour. Everyone of us knows what is intended for behaviour and most people think it is the typical matter of study for psychologist. This common sense is quite different from what scientists actually consider: indeed according to them, behavior is anything a person or animal does that can be observed and measured [9].

In general terms, behavior is the product of two kinds of variables: biological and environmental. Biological variables include anatomical structures (birds can fly, people can't), normal physiological processes (digestion, respiration, neurological changes resulting from experience), and anomalies in anatomy and physiology due to injury or disease. Also genes influence behavior, although indirectly, through their effects on anatomy and physiology.



Environmental variables include any changes in the environment (a rise in temperature, the availability of food, comments by other people, cultural customs). Behavioural analysis finally tries to understand, describe and predict behavior analyzing it in terms of interactions between the biological causes and the environment [9, 10].

The study of the behaviour is both intellectually challenging and practically important and although it aims generally at the understanding of natural principles [11], most scientists try to pursue medical research outcomes (even as long-term results): Genetics, Neuroscience, but also more clinical medical branches like Neuro-rehabilitation make a wide use of behavioural analysis as an instrument to investigate how the human body physiologically works and to explore the causes and evaluate the possible treatments of pathological conditions. The usefulness of such an approach to the research is highlighted by Martin [11]: indeed even the complete knowledge and the understanding of the underlying biological or genetic mechanisms is not sufficient to totally and completely describe and then predict the complex outcoming behaviour of an animal or human.

1.1.1 Behavioural Phenotyping

Ever since Gregor Mendel used the observable traits of pea plants to define and follow units of genetic inheritance, the definition and testing of phenotypes has had a key role in genetic analysis. *Phenotypes* are the expression of genotypes and indeed they reveal gene function. In this regard, phenotypes are an essential intermediate in the pathway from basic genetics to biological understanding [12]. A clear and widely shared definition of behavioural phenotyping lacks: Crawley, referring to a mouse, defined it as “*the complete characterization of the mutant mouse line on behavioral tests designed to address the hypothesized functions of the product of the targeted gene*” [13], Harris proposed that “*behavioral phenotypes are stereotypic patterns of behavior that are reliably identified in groups of individuals with known neurodevelopmental disorders and are not learned*” [17, 16], while Flint and Yule, including the characteristic types of behaviors, proposed that “*the behavioral phenotype is a characteristic pattern of motor, cognitive, linguistic, and social abnormalities that is consistently associated with a biological disorder*” [18].

However there is a clear convergent acknowledgement on the growing importance of behavioural phenotyping. Many scientists are coming to the conclusion that advances in genetic and genomic analysis are being hindered by the slow pace at which our understanding of biology (that is, phenotype) is



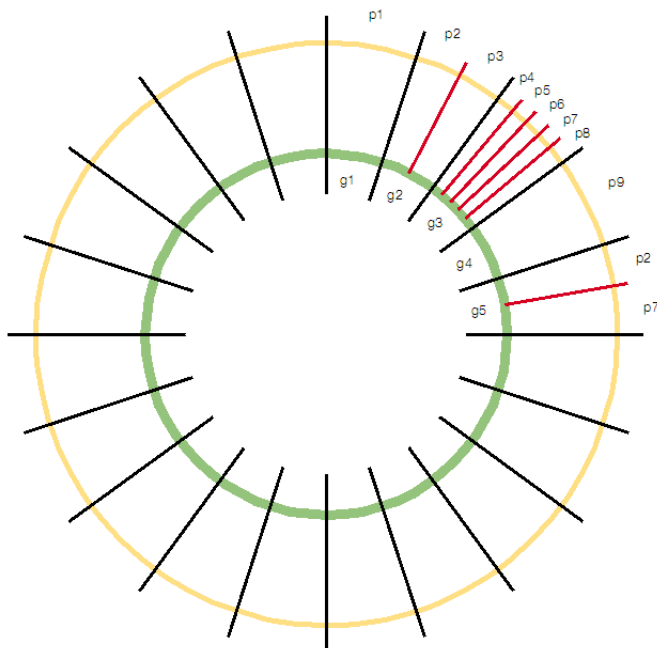


Figure 1.1: A phenotypic map (yellow) can be generated to correspond to any genomic map (green). Some genes, such as gene1 (g1), have only one corresponding phenotype (p1), whereas most genes have many corresponding phenotypes. Phenotypes can be coded for by more than one gene, as shown by p2, which is affected by g2 and g5.

progressing [12]. In 1996, Brown and Peters called attention to 'the phenotype gap' in mouse research compared to the massive amounts of genetic data being obtained [19]. This explains the current trend in Genomic research to produce the so-called 'phenomic map' (conceptually shown in Fig.1.1).

As an example for *Escherichia coli* around 1.000 phenotypes have been tabulated that correspond to various genes that have been studied. Of course in diploid and higher organisms this will be complicated by the fact that several genes can affect gene expression, and the resulting phenotypes of each other, leading to epistasis, complex traits and multifactorial diseases.

Giuseppe Cavallo

1.1.2 The animal models

As briefly stated above, most efforts in research regard the prevention or the effective treatment of human affecting pathologies aiming more generally at the improvement of human life. Under this perspective behavioural analysis gives its own contribute: the search for behavioural phenotypes in animal models is mostly guided by behavioural anomalies that have been observed in human disorders. Many neuroscientific researches use biological (animal) models for testing their hypothesis on neurodevelopment, social behaviors, reproduction, feeding, motor functions, sensory abilities, emotional responsivity, learning, and memory [21, 20, 17, 14]. The most used animal models are mice and rats: there are many studies on them using neuroanatomical, electrophysiological and pharmacological approaches to dissect behavioural traits and the neural systems that underlie them [19, 21, 20, 23, 32, 31].

The mouse is especially important as a model organism for behavioural studies because of the ability to manipulate its genome and to observe the resulting phenotypic consequences using molecular, cellular and electrophysiological approaches.

In order to determine the genetic or molecular basis of neurological diseases, it is first necessary to translate the phenotype 'abnormal behaviour' into measures that can be assessed in animal experiments (testable measures). Clearly, psychiatric symptoms cannot always easily be translated into behaviours that can be defined and operationalised in animal models.

One solution is to break down the symptomatology into elemental phenotypes that can be individually tested in both human populations and animal studies [14]. This approach reduces the time wasted for the analysis by simplifying it as much as possible, but it presents a big fault: it assumes that a complex behaviour (related also to environmental parameters) can be fully described by a single measure of a particular parameter. Furthermore often the assessment of a behaviour is performed qualitatively by visual inspection of researchers (i.e. typically using videocameras), making thus the whole measurement totally subjective and depending on the particular conditions of the test. Most experiments on behaviour presented in literature use such methods [25, 26, 27].

Another important aspect was stressed by Gerlai [24] with the scientific discussion on the "ecology" (i.e. ecological means unstructured and as natural as possible [28]) of the environment of the experimental tests. Infact it is clear that environment strongly affects behaviour so that it is hard (if not impossible) to dissect whether a particular aspect derive from genetic (internal) mechanisms or from environmental (external) conditions. So if one is interested in discover-



ing new biological mechanisms or understanding how and what genes express, it is crucial to filter all influences derived from the external environment in order to focus only on those changes and effects generated by internal causes.

A real improvement of the situation could derive from technology; with the rapid development of the new mechatronic technologies and the progressive integration of engineering in medical fields, innovative alternative methods have been proposed to overcome current difficulties. The keyword of the new approach is “multimodality”. Gerlai in [24] proposed technological devices which are able to increase the information density of the test (i.e. to increase the number of behavioral measures of brain function one can obtain from a single test) and to increase the flexibility of the test apparatus, so that it can tap into a broader spectrum of brain functions. In this way the researcher is allowed to monitor and study several physiological and environmental parameters in a single test and to perform test batteries in series as already suggested by Crawler [23] and van der Staay [14]. Mechatronics can provide also a solution to the need of an ecological environment. Indeed the development of MEMS (Micro Electro-Mechanical systems) enabled the strong reduction of the weight, the dimensions and, in general, of the obtrusivity of the sensors. Infact MEMS can be used, as shown in many experiments present in literature, as wearable (sometimes even wireless) systems expanding the possibility of testing animal models or even human in their really natural living conditions.

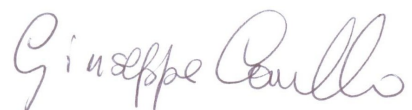
1.2 The mechatronic paradigm

As shown in previous sections, behavioural analysis has a very wide fields of application and the use of innovative technological devices could enhance greatly the outcoming results. In this work the author explored the possible integration between behavioural analysis and Mechatronics

Different definitions of Mechatronics have been published both on papers or books. As an example, the definition given by IRDAC (Industrial R&D Advisory Committee) of the European Community is the following:

“The term Mechatronics refers to a synergistic combination of precision engineering, electronic control and systems thinking in the design of products and manufacturing processes. It is an interdisciplinary subject that both draws on the constituent disciplines and includes subjects not normally associated with one of the above.” [1]

Van Amerong [2] instead focused on the major benefits that a mechatronic approach could produce; indeed he stated that respect to classically designed



devices, mechatronic systems:

- have greater flexibility
- have a better performance and higher quality
- are less expensive

Other definitions affirm that “*Mechatronics is the synergistic combination of mechanical and electrical engineering, computer science, and information technology, which includes control systems as well as numerical methods used to design products with built-in intelligence*” [4]. However a final conclusion has been provided by Hewitt [5] who said that a precise definition of Mechatronics is not possible, nor is it particularly desirable, because the field is new and expanding rapidly; too rigid a definition would be constraining and limiting and that is precisely what is not wanted at present.

According to the previous definitions, Mechatronics cannot be considered simply as a new research field or a new engineering branch; it is a novel way of conceiving and designing devices applying theoretical concepts and integrating technologies and skills from different scientific fields sometimes apparently totally unconnected.

The scientific roots of Mechatronics derive from the growing awareness in the scientific community that the technology cannot be separated according to conventional disciplines and further that important innovations often stem from the interaction of several previously unconnected streams of scientific and technological activity [6, 7].

As biomedical engineers, it is worth also to name Biomechatronics. Biomechatronics is using biomedical knowledge for the development and optimization of mechatronic systems. This covers bionics (biology for engineering) as well as biomedical engineering and its relatives (engineering for biology) [8, 2]. So the relation between the “bio”-world (biology, genetics, medical science) and engineering is twofold: one can use physiology, biology or neuroscience principles as a source of inspiration to design innovative more performing devices or control systems; the inverse process is to put engineering techniques and methods to use in medical science for the development of new tools aiming at both base research or clinical practice in medical disciplines.



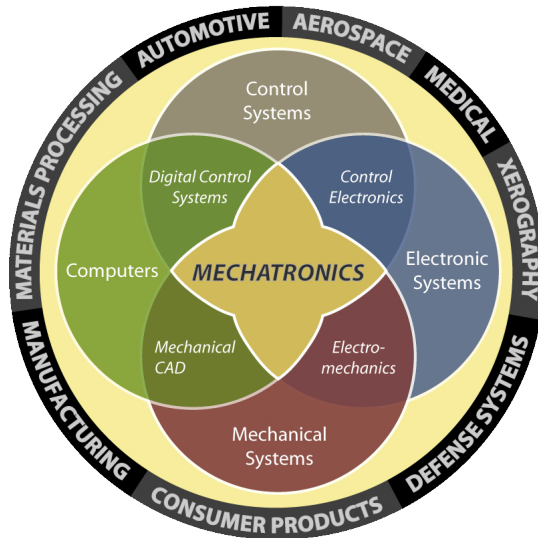


Figure 1.2: The integrated approach of multidisciplinary features brings to Mechatronics, which integrates many engineering fields to the development of innovative products in several commercial areas.

1.3 The proposed approach

Fig.1.3 summarizes the structure of the research done. In particular Behavioural Analysis is generally performed on humans or on animal models. Animals (mostly mice and rats, but also primates and other) are widely used for basic research in Neuroscience or Phenomics as model of particular human features or pathologies. In basic research also human subjects (both healthy or pathological) can be matter of study to identify the biological mechanisms underlying the behaviours detected. Behaviour can be also study for diagnosis purpose so to understand and correlate motor abnormalities to cognitive impairments or diseases. Of course in this case behavioural analysis can be applied only to human. The last application presented in the scheme is performed only on human and concerns the use of behavioral analysis through mechatronics to assess neurological conditions of patients and to define a measurement scale of 'distance to normality' useful for clinical evaluation in neurorehabilitation.

So the following chapters will present different case-studies related to this

Giuseppe Cavallo

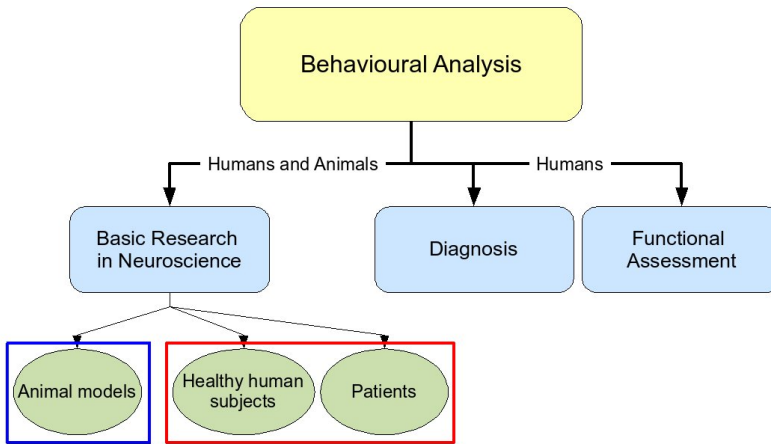


Figure 1.3: The possible application of behavioural analysis: the blocks represent the single research activities performed during the PhD and reported in this thesis

schema showing the improvements and the benefits that the mechatronic approach implies.

The second chapter is devoted to the study of a force detecting platform for tremor detection in mice model of behavioural disorders. In this case the mouse to be analyzed can move freely and the behavioural analysis is performed during the movement.

The third chapter presents a mechatronic platform for the assessment of motor performances in both healthy or impaired subjects. The platform allows the analysis of a planar catching task of a sliding object. The platform is completely modular and one possible application concerns the investigation of the activation of motor cortex areas and the neural motor organization and planning before the movement initiation.

The fourth chapter shows how behavioural analysis can be applied to early diagnose neurodevelopmental diseases such as the Autism by linking abnormalities detected in motor domain to cognitive impairments. This is the main topic of Neurodevelopmental Engineering, that will be presented in the chapter.

Giuseppe Cavallo

The fifth chapter illustrates an application of behavioural analysis on human, in particular in post-stroke subjects. The chapter presents some techniques for the extraction useful clinical features as markers to assess a recovery process. Measurements in this case are performed on an isometric force detecting platform, so that no movement is executed by the patient during the analysis.

Giuseppe Cavallo

Tesi di dottorato in Ingegneria Biomedica, di Giuseppe Cavallo,
discussa presso l'Università Campus Bio-Medico di Roma in data 08/02/2008.
La disseminazione e la riproduzione di questo documento sono consentite per scopi di didattica e ricerca,
a condizione che ne venga citata la fonte.

Giuseppe Cavallo

Chapter 2

A tremor detecting platform

Movement and behavior analysis is a key research area in the domain of biomedical engineering and in many other medical research domains aiming at the understanding of physiological motor and cognitive basic mechanisms. The systematic application of robotic and mechatronic technologies to realize new tools and measurement methods for quantitatively assessing motor and cognitive functions in humans as well as in animal models is gaining an increasing popularity.

2.1 Introduction

Biomedical Robotics is a discipline in rapid and continuous development. It aims at providing innovative methods and tools for improving the quality of health care but also for enabling new research pathways in the medical and biological domain. An increasing research interest is growing worldwide, both in the medical and in the engineering community, on the potential impact of the application of robotics to the field of Neuroscience (Neuro-Robotics) [41], [42].

This work is a first significant attempt to link the application of mechatronic and robotic technologies to specific areas of Neuroscience, such as neurobiology and neurophysiology of developmental disorders, which have been only partially addressed so far by roboticists. This new area could be dubbed Neuro-Developmental Engineering. More specifically, the multidisciplinary research work that is being carried out by a joint team of roboticists and neurobiologists is focusing on the introduction of such technologies in the area of Phenomics.

Phenomics is a new promising discipline which integrates and expands genomic research [43]. It analyzes the relationship between genetic code and its external expressions, i.e. phenotype, in order to better understand physiological and neuro-physiological mechanisms. Phenomics frontiers are still not well defined; one of its principal trends is represented by behavioral analysis, in particular movement and gait, in animal models. The aim of this research is finding some characteristics in animal models that could be compared with patterns of physiological or pathological human models. A particular mouse model, the Reeler, seems to be particularly related to human neuro-developmental disorders such Autism Spectrum Disorder (ASD). The Reelers are spontaneous mutant mice that present evident tremor and ataxia, i.e. the loss of the ability to coordinate muscular movement. A quantitative and objective analysis of tremor would provide useful, for example, when evaluating pharmacological treatment.

2.2 Rationale

Animal models (i.e. mutant rodents) are widely used in Neuroscience aiming at the understanding of physiological or pathological mechanism of the brain and CNS and their development [38]. Experiments on animal models allow the researchers to access directly on biological data and, through appropriate scaling, to compare these results on human.

Advances in genetic technologies have permitted the identification of genes disrupted in many mutants, allowing a molecular interpretation of the phenotypes. For several decades, the spontaneous mutant mouse reeler has been used as a model for the analysis of the development of laminated brain structures.

Recently, *reelin*, the gene disrupted in the reeler mouse, has been identified. *reelin* encodes a novel extracellular molecule that controls neural cell positioning through mechanisms that are not yet completely understood. Analysis of the expression pattern and the properties of the reelin gene product (Reelin) suggests models for its function during brain development [38]. Scaling these new findings to human, the Reelin glycoprotein is implicated in the etiology of several neurodevelopmental disorders ie, schizophrenia,[33], [34] bipolar disorder, major depression,[34] and autism.[35], [36]. Moreover, converging data point to Reelin as an important modulator of a neuronal signaling system that may be involved in synaptic transmission and plasticity [37].

Reeler is an autosomal recessive mutant mouse that was first discovered nearly 50 years ago[62]. This mutation produced an ataxic and reeling gait in the affected mice. Analysis of the central nervous system in the mutant



mouse revealed multiple defects such as inverted cortical lamination, abnormal positioning of neurons and aberrant orientation of cell bodies and fibers [62], [39].

The Reeler is an autosomal recessive mutation; heterozygous mice are indistinguishable from normal, whereas homozygous mice exhibit ataxia, tremors, imbalance, and a typical reeling gait that becomes apparent at 2 weeks after birth [38].

The human reelin gene (RELN) has been cloned and mapped to chromosome 7q22. Its product is similar to mouse Reelin (94.2%identity), suggesting a highly conserved function. RELN is expressed in the brain before and after birth, at the highest levels in the cerebellum [40].

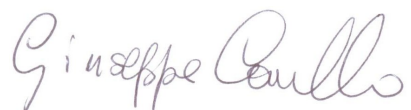
Whether Reelin is involved in a human disease or not, it is important to recognize that many neurological disorders, including schizophrenia, autism and some forms of childhood epilepsy, arise as a consequence of migratory defects during brain development. Thus, it is possible that an analysis of the molecular and cellular basis and of the phenotype of Reelin function may reveal important information about the mechanisms responsible for these devastating diseases.

2.3 The force platform

Earliest attempts of quantitative analysis date back to 1989 when Steinberg [44] studied mouse ataxia by analyzing footprints via a digitizer tablet for successive computer based analysis. Most recent approaches make use of available technology which allows assessing both kinematic and dynamometric data. Force platforms, mainly consisting of a rigid large platform suspended upon lateral load cells, have been developed [45], [46], [47], [48] to analyze the overall Ground Reaction Force (GRF) during locomotion. Kinematics relative to a single paw could be derived by means of a camera located beneath the (transparent) platform. To the authors knowledge, only rare examples, such as [49], [63], can be found in literature where the GRF relative to a single paw can be determined.

Another recent application is the mechatronic system for behavioural and gait analysis in animal models presented as a tool for robot-mediated rehabilitation [64].

Tremor characterization and evaluation is classically performed by using assessment scale based on the researcher's observations and thus being subjective and low repeatable. With the development of electronics and computer



science, several devices for tremor detection and analysis have been developing [73]; they are generally based on electromyography detection [50, 52, 56, 57], accelerometers [58, 59, 56], force transducers [60, 61], measurement of linear and angular displacement [53, 54], measurement of velocity [55, 56] and video recording [51].

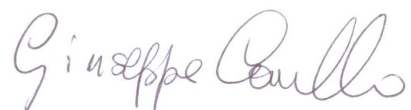
Some tools are even commercially available such as Smartcube (PsychoGenics Inc.) and IntelliCage (NewBehavior Inc.) [43], consist of sensorised cages which allow to automatically capture, quantify and store information on a large number of behavioral motor and posture patterns but they do not provide information of GRF relative to a single paw during locomotion. As for commercially available sensors, given the specific needs of this application, it is very difficult to find multiaxis force sensors matching the geometric constraints or which can be adapted to suit such needs. The few suitable sensors are either based on complex mechanisms, in terms of fabrication technology, or on complex signal processing electronics. In both cases such solutions become more and more unsuitable to scenarios where many of these sensorised modules are combined together, as described below.

2.4 Functional and technical specifications

The aim of this work is providing neuroscientists with a force sensor, able to detect tremor from small animal models i.e. reeler mice. In order to plan and realize this device, functional specifications about the kind of analysis to be performed, the dimension and the strength of the animal model and the environmental conditions were gathered directly from the neuroscientists working to the Developmental Neuroscience and Neural Plasticity Lab at Campus Bio-Medico University and afterward translated into technical constraints.

For what concerns the functional specifications, first of all it is necessary the platform to be highly specific to paw tremor rather than to whole body tremor as in [65]. This issue can be achieved by reducing the size of the sensing element to be comparable with a single paw of the animal. This first feature opens the way to a series of possibility in the design of the tool: a small dimension sensing element can be simply placed side by side with other small sensing elements around the arena the animal should be posed on.

Following this preliminary directions, the device could be thought as an arena (i.e. a cage) whose surface contains one or more force sensors the mouse can step on. Such a platform, from the mouse perspective, should look pretty much like a tile in the floor. This would allow to patch the floor with a variable



number of sensorised tiles for different kinds of experiments, allowing reconfigurable modular setups. A direct consequence of the use of multiple tiles is that each force sensor should be mechanically simple and robust, so implying the low-cost of the structure.

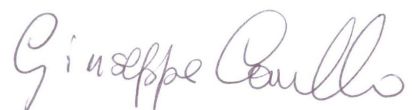
The mechanical simplicity is also a desirable feature because it should be considered that this tool aims at being extensively used in non-engineering laboratories and so it should allow simple assembly from off-the-shelf components. All these considerations exclude definitively the use of complex mechanical structures.

Through the analysis of the literature about GRFs exerted by animal models during normal gait, it can be seen that, due to the weight of the animal, the vertical GRF component is generally ten times larger than the horizontal ones [49], [63]. For this reason, it is suitable to use different sensors in the two cases. In particular, normal forces besides being larger in magnitude, are easily measured via pressure sensors, e.g. piezoresistive arrays, directly placed on top of the tile. In this way the pressure distribution can also be derived, providing thus extra information, e.g. the heading direction, which can be correlated with the in-plane components. On the contrary, detection of in-plane forces requires an “ad hoc” design and it would have a major scientific interest since in literature tremor analysis via horizontal GRFs detection has not been explored sufficiently as well.

Although the research tool this paper deals with is able to detect only dynamometric data, other approaches can be found in literature for the development of detecting tremor devices ([46], [47]) making use of available technology which allows assessing both kinematic and dynamometric data. In those works, force platforms, mainly consisting of a rigid large platform suspended upon lateral load cells, have been used to obtain dynamometric data during locomotion whereas kinematics relative to a single paw could be derived by means of a camera located beneath the (transparent) platform or an external camera taking an environmental view.

Another functional aspect that came out after the first prototypes is the need of knowing which body part of the mouse is in fact interacting with the tile and where the mouse paw is headed during the interaction. A camera just beneath the sensorized tile (made of a transparent light material, i.e. Plexiglas) was placed in order to solve this issue; in this way through an offline data elaboration it is possible to drop the artifact of the experimental session, focusing the analysis just on the scientifically relevant part of the signals.

Finally a very important feature was added to the platform. As mentioned above, the GRF detecting tool should be used in a Neuroscientific lab. This



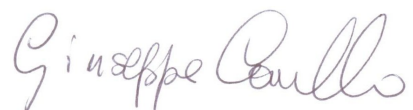
means that a very simple calibration procedure to be performed just before each experimental session would guarantee the maximum reliability of the measurements. Usually calibration procedures are time consuming and require very good instrumentations and structured environments. A novel *sensor fusion* procedure was experimented to overcome these limitations. In particular the platform was provided with an acceleration sensor which detects the horizontal accelerations of the sensorized element. To calibrate the device, it is just needed to provide an impulse-like input (small mechanical shock) to the platform, thus obtaining a double information of the system response. Through data elaboration techniques, the calibration curve of the platform can be finally derived.

2.5 Design of the platform

As previously mentioned, the interaction between engineers and neuroscientists played a fundamental role in the design and the development of the device. During the designing phase, for instance, a continuous bi-directional flow of information was exchanged between them: at first functional specifications were collected by engineers from neuroscientists; then engineers translated them into technical constraints (such as the maximum applied strength, maximum allowable displacements, etc.), elaborated different solutions and chose the one that better matched with medical and practical needs and criteria. Finally, once the sensor has been developed and tested, neuroscientists gave to designers important feedbacks useful to improve the system in further developments.

The final device will be a mechatronic platform for behavioural analysis purpose, composed by a sensing stage (tremor, temperature, position, orientation detection) and an actuated stage in order to perform also interactive tests with mice as general as possible, by supplying them different kind of stimuli. In this paper the first sensing stage is presented in its planning and realization.

Generally forces can only be determined via indirect measurements [66]. Typically, load cells perform force measurement via two levels of transduction. The *primary transducer* consists of an elastic mechanism which undergoes deformation under the action of force. A *secondary transducer* is then used to transform the mechanical deformation into an electrical signal. Once the maximum force to be measured is given, the elastic mechanism is designed to remain within the linear range, which usually requires high stiffness.



2.5.1 Primary transducers

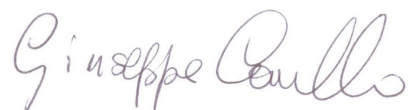
In general, for a given material, the stiffer the structure, the larger the force it can withstand; on the other hand, considering the secondary transducer, high stiffness directly translates into small deformation, i.e. increasing stiffness negatively affects resolution and sensitivity. Finally, the mechanical stiffness will be determined as a trade-off between the need for not-too-compliant structures and the need for resolution. Nevertheless, when both stiffness and resolution are hard constraints, solutions can still be found by means of complex mechanical structures. For example, instead of using bending cantilever with homogeneous cross-section as primary transducer, just narrowing the beam at specific points [67] allows concentrating deformations at those very points, therefore increasing sensitivity, without changing the overall stiffness. Of course, these solutions require higher costs for fabrication and assembly, reducing the simplicity of the overall system and must be rejected due to motivations described in section 2.4.

Again according to functional specifications, only horizontal components of GRFs are interesting for this application, while the vertical one must be neglected. This issue can be faced and solved through a smart mechanical design, i.e. *the parallel kinematism*.

The parallel kinematism adopted in this work has been obtained by clamping two tiles to the ends of four pillars, so that the two tiles are constrained to move parallelly one another for small deflections; this achievement makes the structure very stiff in the axial (vertical) direction, but relatively compliant in the other two transverse (horizontal) directions intrinsically allowing horizontal displacements detection more than vertical one. This means that effects of vertical forces are negligible in comparison to those of the horizontal ones, normal forces¹ and torques have in fact negligible effects.

Design and fabrication of the tiles, being rigid elements, poses very little problems. Figure 2.1 shows the structure of the platform. The large central hole simply reduces the total weight, increasing thus the sensor bandwidth. The four smaller holes require more precision since pillars will be inserted through such holes and glued for clamping. On the other hand, pillars require much more care. They represent the compliant part of the mechanism and therefore

¹Even considering axially rigid pillars, normal forces are counterbalanced only if the top tile is perfectly centered. In case of a lateral shift, the pillar axis does not coincide with the vertical direction and therefore normal forces will have an effect. Such effect is proportional to the lateral deformation to the length of the pillars ratio, i.e. it can be reduced by increasing the stiffness of the pillars.



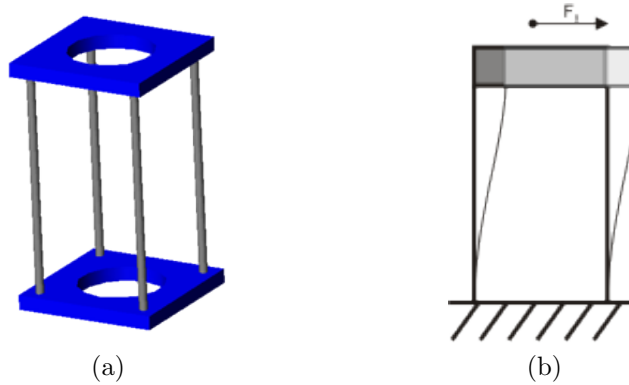


Figure 2.1: The mechanical structure of the sensor consisting of two tiles (central holes simply reduce mass) kept parallel by four long and thin pillars (a). Each pillar has both ends constrained to be perpendicular to the tiles. Long and thin pillars are used to provide enough compliance in the transversal direction while being extremely stiff in the axial direction, therefore only in-plane forces cause detectable deformation (b). By clamping the bottom tile to the ground, the top one is constrained to move parallelly to the ground, i.e. the structure is practically not deformed by weight forces and torques.

final stiffness will pretty much depend upon their geometrical features. Good repeatability is guaranteed by the use of commercially available needles. Four stainless steel needles for spinal anesthesia (BBRAUN Pencan) were used. This is at the same time an extremely inexpensive and accurate solution since needles manufacturer must respect ISO standards (9626). Furthermore hollow structures are to be preferred to solid ones since, for the same bending stiffness, hollow structures are lighter, increasing thus the sensor bandwidth. Pillars, i.e. needles, are clamped at both ends to the rigid tiles. By means of elastic beams theory, the relation between lateral, i.e. horizontal, displacement and horizontal force F_0 is:

$$\delta = \frac{L^3}{12EI} F_0 \quad (2.1)$$

where E is the Young's module and I is the moment of inertia which, for a hollow cylinder with inner and outer radius respectively r_i and r_o , is given by

Giuseppe Cavallo

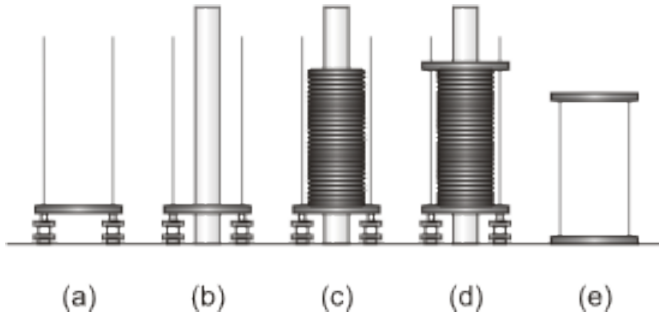


Figure 2.2: The self-aligned assembly procedure. Four needles are inserted in the small through holes of the tile and placed in the upright position (a). A centering cylinder is placed through the central hole of the tile (b). Spacing discs are then piled up (c) as the cylinder keeps everything up and steady. When a given number of discs is piled up, the second tile is also inserted (d). After each end of the needles has been glued to the tiles, first the cylinder is removed, then the discs are let slide sideways and then, after cutting off protruding parts of the needles, the structure (e) is finally assembled.

$$I = \pi \frac{r_o^4 - r_i^4}{4} \quad (2.2)$$

The choice of needles dimensions will thus affect the stiffness and therefore resonance frequency as well as the bandwidth of the structure.

The maximum horizontal force expected for a laboratory mouse was estimated, see experimental results in [49], [63], to stay below $F_{max} = 0.1 N$, assuming as F_{max} the normal force that each paw sustains (around a quarter of the mouse weight). A mouse stepping on the platform should not perceive any compliance in the tile in order to keep the experimental environment as “ecological” as possible avoiding unnatural behaviors of the animal. For this reason, the maximum lateral displacement displayed by the tile was heuristically² set to be $\max \delta_{max} = 100 \mu m$. Maximum displacement should only occur when the maximum lateral force is applied, leading thus to a lateral stiffness $k_{tot} = 4 \times k_{needle} = 1000 N/m$. Each needle³ shall then display a stiffness

²100 μm can be considered a negligible displacement with respect to the animal’s paw.

³Needles are mechanically in parallel, therefore the final stiffness will be four times the stiffness of a single needle

Giuseppe Cavallo

$k_{needle} = 250 \text{ N/m}$. When selecting a needle from a catalog, a gauge must be specified in order to define parameters such as inner and outer diameter. For this application, a gauge $G = 25$ was chosen, corresponding to inner and outer diameter respectively $r_i = 0.51 \text{ mm}$ and $r_o = 0.26 \text{ mm}$. Needles are made of stainless steel, i.e. Young's module $E = 200 \text{ GPa}$. Considering the weight⁴ of the aluminum tile ($\rho_{al} = 2700 \text{ Kg/m}^3$ is the aluminum mass density) of about $M_{tile} = 0.0012 \text{ Kg}$ and the total stiffness of 1000 N/m , a first resonance can be estimated at about $f_0 = K_{tot}/M_{tile} \approx 114 \text{ Hz}$, i.e. well beyond specifications.

Assembly is another important aspect in choosing mechanisms of the sensors or sensing techniques. Special care was taken in designing the sensor in such a way that a self-aligned assembly procedure was eventually possible. Self-alignment in fact guarantees repeatability. Figure 2.2 shows the assembly steps. Four needles are first inserted in the through holes (the smaller ones) of the tile and placed in the upright position. The central hole of the tile, besides reducing the final mass, allows insertion of a centering cylinder, i.e. this will constrain every part to stay centered with respect to the axis of the cylinder itself. In order to have a pre-determined distance between the two tiles, 2 mm thick discs, used as adjustable spacers, were piled up. Once the exact number of discs is inserted, the second tile is also put in place. So far, only gravity helped maintaining everything aligned. At this point, needles can be glued at both ends to the tiles. Once the glue is cured, the cylinders and the spacers (discs) can be easily removed while protruding parts of the needles can be simply cut off. A self-aligned structure is thus obtained.

Finally, since the platform will be used to detect tremor i.e. a dynamic signal, it is necessary to define the maximum frequency the sensor should be able to detect and then try to keep the sensor's resonance frequency faraway from it. Tremor, whether natural or pharmacologically induced [68], never exceeds 30 Hz and therefore a 100 Hz structural resonance will induce a practically flat response of the system in the range of interest ($0 - 30 \text{ Hz}$).

Main characteristics of the force platform, or tile, may be summarized as follows:

kinematics: being interested in only detecting the in-plane components of the GRF, the tile should be kinematically constrained to stay parallel to ground.

mechanism: in order to sense in-plane forces, the (rigid) tile should be me-

⁴The equivalent, i.e. for resonance purposes, mass of the needles is negligible with respect to the tile



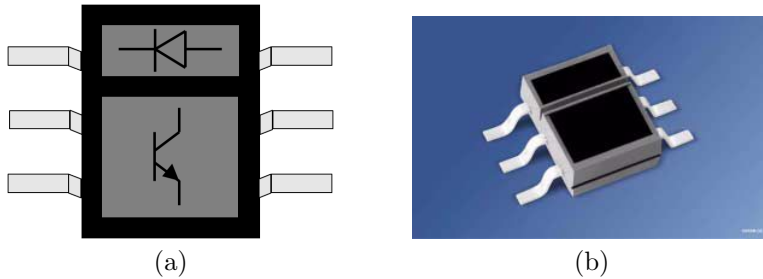


Figure 2.3: Functional schema (a) and picture (b) of the IR optical proximity sensor

chanically connected to the ground via an elastic mechanism that displays a certain compliance in the in-plane directions while being extremely stiff in the vertical direction.

dynamics: the (rigid) tile plus the compliant mechanism behave as an oscillating system whose resonant frequency should be higher than the typical frequencies characterizing tremor.

2.5.2 Secondary transducer

Since only compliant structures as simple as homogeneous cross-section bending beams will be considered, stresses and strains will be pretty much distributed. Deployment of strain gauges is therefore not advisable, high stiffness constraint leads to small deformations and strains. Preliminary calculation have shown that at maximum exerted forces strains would be in the order of microstrains, therefore noise would represent a major issue. As an alternative, non-contact proximity sensors were considered. Among several other choices, IR reflective sensors turned out the best choice in terms of complexity and cost reduction.

In particular, an OMRON OPB706B and OMRON SFH 9201 were used where an infrared (IR) emitting diode and a phototransistor are mounted side by side and embedded in the same plastic case (Fig.2.3). The phototransistor responds to radiation from the emitter only when a reflective object passes within its fields of view, about 10 mm for the selected sensor.

For proximity measurements, emitter and receiver simply face a side of the tile, the gap between the optical sensor and the (top) tile is thus detected as the tile moves as a consequence of exerted in-plane forces. The optical

Giuseppe Cavallo

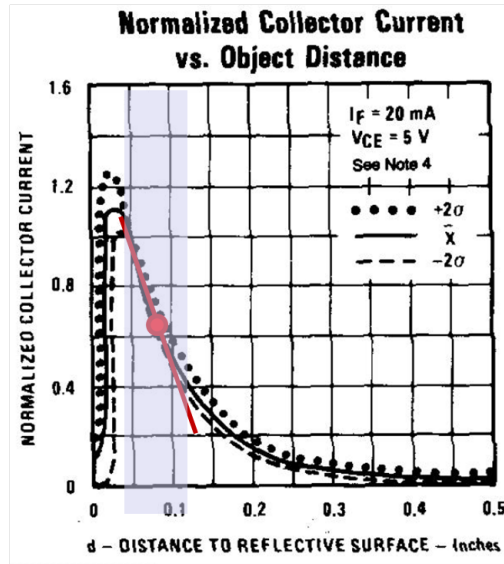


Figure 2.4: The optical retro-reflective IR proximity sensor calibration curve is highly non-linear, but it can be linearized under the hypothesis of small displacement (i.e. $\pm 100 \mu\text{m}$)

sensor produces a current variation in response to a mechanical deformation. The response is shown in fig.2.4: it is a highly nonlinear curve, but for small displacements it can be easily linearized in some particular points. Fig.2.4 shows one linearization point.

The optical sensor needs of a power supply and output signal control electronic circuit: a current-voltage (I/V) converter (i.e. a pre-amplifier stage) is used to generate a voltage from the original current signal; in this way it can then be filtered and amplified for numerical (A/D) conversion. Then a low-pass filter (100 Hz) and offset regulation stage is added to the circuit. Finally the signal is further on amplified and sent to the A/D module.

In order to read out both components of GRF, two optical sensors were used which faced different sides of the tile. A National Instrument ADC board was used for a 12 bits A/D conversion of signals coming from the two sensors and for a serial transmission to a Personal Computer (PC) via an USB connection. The acquired signals were thus stored for later processing.

Giuseppe Cavallo

2.6 Experimental setup and calibration

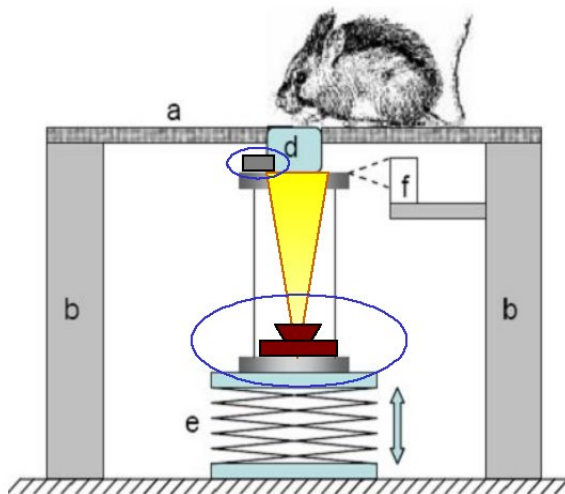


Figure 2.5: Experimental setup

In order to test the force platform with laboratory mice, a simple apparatus was set up as in the following. With reference to Figure 2.5, a circular arena (15 cm in diameter) with wooden floor (a) was placed at a certain height from a table and sustained with lateral columns (b). At the center of the floor, a 1.5 cm diameter hole was drilled which would host the sensorised tile (d), i.e. a plastic cylinder glued on top of the force platform (c). By means of a manual z-axis stage (e) placed right beneath the wooden arena, the force platform was lifted up so that the plastic cylinder would fit through the hole in the center of the arena and stay right at the level of the arena. The optical sensor (f) was fixed at a height so that it faced one side of the platform. Different versions of the platform were developed, in further improvements of the burden, the shape, the handiness and the modularity.

Preliminary tests were made using only one optical sensor, obtaining only data from one of the two GRF components, even if the overall system has been completely designed and developed to perform 2 DOF analysis.

Before calibrating the whole system, the optical sensor's characteristics were also verified with respect to the operating environment. Optical sensors based

Giuseppe Cavallo

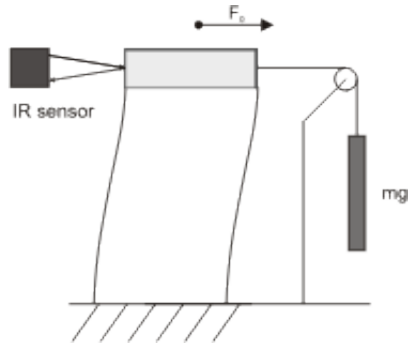


Figure 2.6: Calibration setup

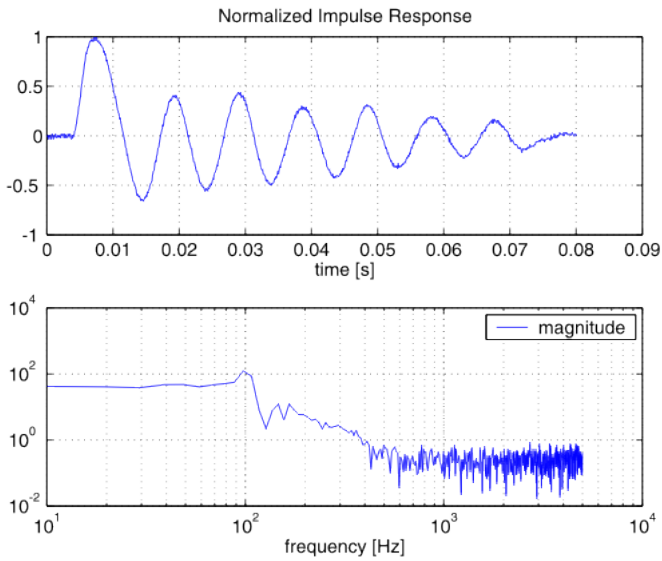


Figure 2.7: Time plot (top) and frequency plot (bottom) of the normalized impulse response of the mechanical structure.

on reflective targets behave differently according to the color and size of the object itself (in this case a 2 mm thick aluminum tile) and surrounding objects

Giuseppe Cavallo

as well. In order to evaluate performance, a micrometric screw was used to simulate the effect of forces on the tiles; in this way tiles displacements could be controlled within $10 \mu m$. Good agreement with the datasheet was verified.

2.6.1 Static calibration

Once the working point was established (by fixing the distance between the sensor and the tile), the force sensor was ready to be statically and dynamically calibrated, by linearizing around the point. Weights ($1, 5 g$) were used to exert in-plane forces as shown in figure 2.6. The numerical ratio between the applied force (mg) and the distance variation measured (μm) by the optical sensor was used to measure the stiffness of the whole mechanical structure, in very good agreement with the expected modelled value ($1000 N/m$). Different weights were used to compute stiffness at different loading conditions. The structure proved linear even outside the range of interest.

2.6.2 The dynamic calibration

After the prototypes were developed, a first but significant test was performed. Figure 2.7 shows the response (both in time and frequency) of the mechanical structure after being subjected to a (small) mechanical shock, i.e. its impulse response. A resonant frequency around $100 Hz$ is evident. Resonant frequency is lower than the theoretically estimated one due to the inertial loading of an extra added mass (element d in figure 2.5). Nevertheless, a flat band is displayed in the frequency range of interest ($0 - 30 Hz$).

Although this technique gives an overview in a sight of the dynamic behavior of the system, it can't be considered as a calibration procedure, being a qualitative test. A quick and easy test was designed to allow the researcher to perform a calibration each time a new experimental session starts.

The goal of a calibration process is to obtain the characteristics of the curve (assumed linear) which correlates the input (i.e. displacement or force) and the output (i.e. voltage) of the device. A line is mathematically described by two parameter, i.e. the slope and the intercept. The intercept (offset) can be simply obtained by measuring the working point of the device. What is really needed is the gain (slope) of the line.

In this application the slope is calculated as follows: the acceleration signal is acquired, filtered and integrated twice in order to obtain the position data; these data are the reference vector to be compared to the output optical sensor



signal for the final calibration. In formulas:

$$V_{opt}(t) = G \cdot \Delta x(t) \quad (2.3)$$

$$V_{acc}(t) = C \cdot \Delta \ddot{x}(t) \quad (2.4)$$

where V_{opt} and V_{acc} are respectively the output voltage of the optical sensor and the accelerometer, Δx is the displacement of the tile, C is the known constant of the accelerometer while G is the slope needed.

The basic idea would be to derive the G constant through the double integration of the V_{acc} (i.e. $\Delta \ddot{x}$) obtaining Δx to be substituted in the 2.3, thus deriving G . In formulas:

$$\Delta x(t) = \frac{1}{C} \int \int V_{acc}(\tau) d\tau^2 = \int \int \Delta \ddot{x}(\tau) d\tau^2 \quad (2.5)$$

Unfortunately this way presents some technical problems mostly related to the difficulty to extract displacement data from acceleration ones. In fact this formulation would be valid in the ideal case where no drift errors affected the accelerometer signal. Numerical integration of an acceleration signal presents, instead, a well-known problem just because of the drift affecting the accelerometers; such an error (assumed constant) grows linearly (respectively as a square power) if the signal is once (twice) integrated along the time.

For these reasons, in order to minimize the noise as much as possible, both the acquired optical and acceleration signals are processed with a narrow pass-band filter whose bandwidth is centered just on the resonance peak (w_0) of the system; around that frequency, indeed, the SNR (Signal-to-Noise Ratio) is maximum and the drift error assumed constant (i.e. frequency 0 Hz) is rejected.

With reference to fig.2.8.(a), the output voltage from the optical sensor is plotted versus the displacement vector derived from the elaboration. The cloud of points is clearly arranged on a negative slope line. Through a linear regression, the two parameters of the line can be revealed. The fig.2.8.(b) shows the comparison between the results of the static and the dynamic procedures. The two curves can be considered overlapped, the maximum difference between the two lines (at the two ends) is less than 1% of the full scale.

After the D/A conversion, the sensor could resolve forces in the order of 1 mN and the final platform sensitivity has been proved to be $-1.02 V/N$. See [70], [69], [71] for details.



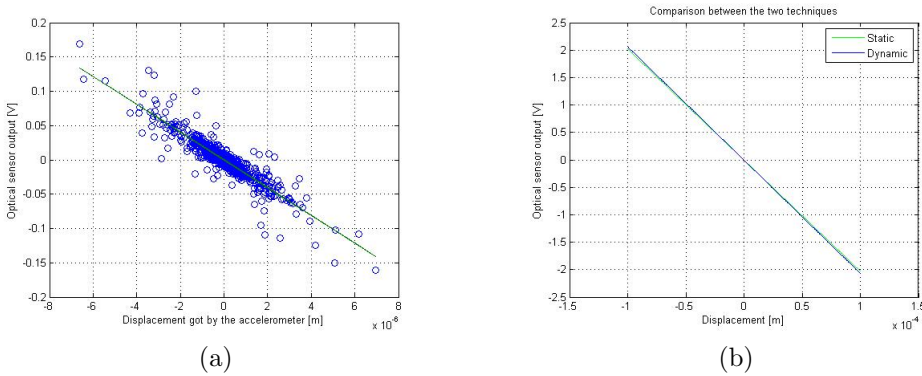


Figure 2.8: Results of the dynamic calibration. (a) V_{opt} vs Δx derived from the double integration of the acceleration signal. (b) The two calibration curves obtained from static and dynamic procedures. The two lines can be considered overlapped

2.7 Preliminary tests and data analysis

Preliminary experimental tests involved 5 mice, 3 reelers and 2 heterozygotes. For each mouse different sessions were performed. All tests lasted between 5 and 10 minutes in order to avoid that emotional factors affected mouse's behavior: it was possible in fact that passing from their cages to the experimental setup environment, mice got nervous or excited; so long lasting tests let them accustom to the new environment and assure that they stepped at least one time on the sensing tile. Furthermore in order to reduce even possible effects of the environmental light on mice behavior, some test has been performed in the dark. The choice of a precise experimental protocol has been particularly difficult because of the few references that can be found in literature. It was noticed that best results were obtained when mouse was free to explore the new environment without particular constraints.

Acquired data were processed in a MATLAB environment. In particular, spectrograms⁵ relative to a wildtype and a reeler mouse are shown in figure 2.9. Spectrograms perform the discrete-time Fourier transform of short-time sliding window. Spikes at different times, in both plots, represent interaction

⁵Windowed discrete-time Fourier transform, see MATLAB function "specgram" help files for details

Giuseppe Cavallo

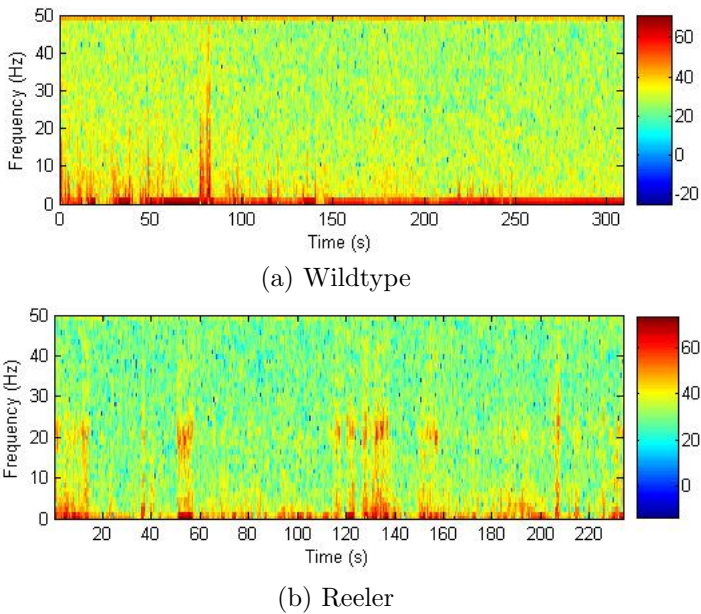


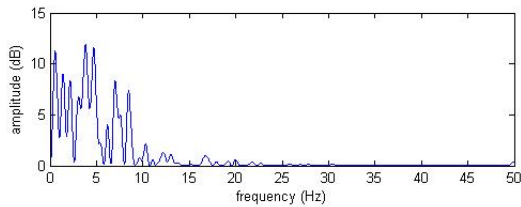
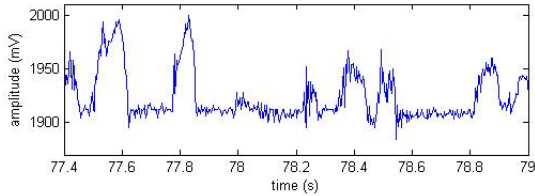
Figure 2.9: Spectrograms for Wildtype (top) and Reeler (bottom) tests. The colored peaks give information on the intensity of the respective frequency component for each time interval

between mouse and platform. The proposed system clearly allows to detect the horizontal band in the 18 – 23 Hz range which characterized the spectrogram relative to the reeler mouse. This means that, as expected, when the reeler mouse steps over the platform, its characteristic tremor is then directly sensed by the platform.

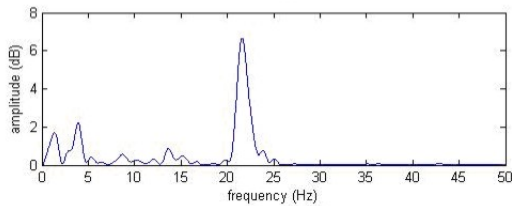
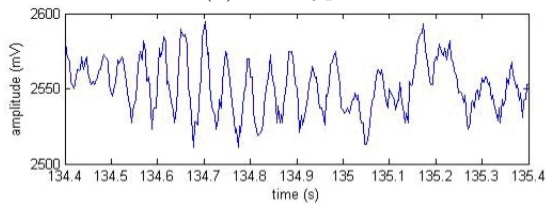
Plots in figure 2.9.(a) and 2.9.(b) represent the so called spectrogram, i.e. a frequency/time representation of signals. The time axis represents the time of the tests (sec). Spikes on the spectrogram occur when the mouse steps on the platform. At first the wildtype spectrogram (figure 2.9.(a)) has been considered: a particular time interval is analyzed (from 77.4 sec to 79 sec); in this interval the colored peak occurs in the spectrogram. In figure 2.10.(a) this interval is analyzed in detail: the upper plot is the acquired signal versus time, the lower plot is its Fast Fourier Transform (FFT). Clearly, no significant

Giuseppe Cavallo

harmonic content is present above 10 Hz. Similar conclusions can be drawn for other time intervals relative to the other wildtype tests as well.



(a) Wildtype



(b) Reeler

Figure 2.10: Plots for Wildtype (top) and Reeler (bottom) tests. The first and the third plot show the time analysis of particularly interesting time intervals while the second and the fourth plot show the corresponding Fourier analysis highlighting the harmonic content of the signals

Giuseppe Cavallo

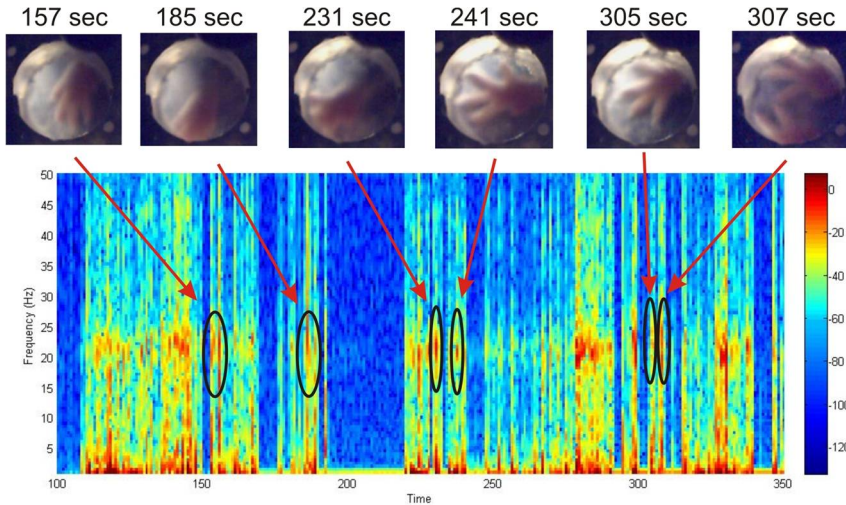


Figure 2.11: A spectrogram related with snapshots taken from the camera. This analysis reveal those very points when the mouse steps on the tile and where it is headed

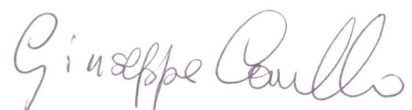
Similar analysis was also performed on Reeler mice tests. From the spectrogram in figure 2.9.(b), relevant time intervals can be found (spikes representing the interactions with the platform), i.e. around 52 – 54 *sec* and 134 – 135 *sec*. One of these intervals is shown in form of time and FFT plots in figure 2.10.(b). In this case, it is clear the presence of (around) 20 *Hz* centered peaks in the spectrum of the signal. This preliminary result demonstrates the effective possibility to use the platform as a detecting tremor device for small animal model.

The fig.2.11 shows a spectrogram correlated with some snapshots taken from the camera beneath the sensorized tile. The use of the camera allows to reject those peaks in the spectrogram where the mouse isn't stepping with its own paws, but it's just touching the platform with some other body parts. This is quite typical in a ataxic mouse. Furthermore the images of the paw could be processed to extract the direction the mouse is heading to, adding more information to the behavioral analysis.

Giuseppe Cavallo

2.8 Conclusion and future developments

In this work a new mechatronic instrument specifically designed for application in the new emerging field of Phenomics has been designed, developed and tested on animal models. In particular the authors attention focused on Reeler mice, a spontaneous mutation that presents traits apparently similar to human neuropathologies like Autism (i.e. stereotypies, tremor). The tight collaboration between neuroscientists and bioengineers allowed the conceptualization of an interactive force detecting platform device that integrates also other kinds of sensors (cameras, pressure and temperature as well as force sensors) as a tool for phenomic investigations and behavioural tests. This paper presents the development of the innovative module for Ground Reaction Force detection for tremor measuring; its novelty, derived from medical needs, is in the capability to sense horizontal forces and in the dimension of the sensing element so to be able to detect even single mouse paw tremor. Also, simple and modular design and fabrication will allow further development of a larger modular, sensorized environment. The sensor is composed by an elastic mechanism, that transforms applied forces in deflection, and an optical stage, that lets to measure the deflection. The whole system has been calibrated and typical characteristics of measuring tools have been deduced such as sensitivity, resolution and frequency response. Then, a series of experimental tests have been performed both on reeler and on wildtype mice. Experimental protocol simply consisted in letting the mouse walk freely on a surface with a hole which hosted the sensorized tile that was able to detect GRF. Data obtained was sent to a PC and elaborated offline in a MATLAB environment. The measurement method, consisting in Fourier analysis with a spectrogram, highlighted that in reeler mice Fourier diagrams a constant peak in frequency at about 20 Hz can be clearly isolated; that means that in time domain an oscillation of 20 Hz can be seen and that oscillation is due to mouse tremor. This tremor can be considered a typical characteristic of reeler disease, since the tests in wildtype do not show any relevant and repetitive peak in frequency. In order to highlight this tremor peak a digital passband filter equivalent to an analogic active one has been developed. Future work will be developed in two main directions: (i) definition and application of new, more structured experimental protocols for assessing the behaviour of the animal model in a variety of situations, e.g. for testing the efficacy of new pharmacological treatments; (ii) implementation of an extended experimental platform, composed by a matrix of the proposed GRF sensors and by other multimodal channels (e.g. cameras, etc.) in order to be able to generate and record many different variables which can be relevant for



Tesi di dottorato in Ingegneria Biomedica, di Giuseppe Cavallo,
discussa presso l'Università Campus Bio-Medico di Roma in data 08/02/2008.
La disseminazione e la riproduzione di questo documento sono consentite per scopi di didattica e ricerca,
a condizione che ne venga citata la fonte.

32

CHAPTER 2. A TREMOR DETECTING PLATFORM

in-depth tremor analysis and identification of other locomotion abnormalities
in small animal models.

Giuseppe Cavallo

Chapter 3

The catching platform

Studies on human motor control are often focused on a specific motion task (opportunately selected) which emphasizes peculiar biological mechanisms that researchers intend to analyze. Catching a moving object, for instance, can be regarded as a natural and ordinary task which allows investigating a variety of issues related to human strategies and synergies, such as kinematics and dynamic analysis of the upper limb during interception and catching, motion prediction, or else generation of internal models in the Central Nervous System (CNS).

A mechatronic system is presented that is conceived to serve as platform for functional assessment of healthy and injured people during tasks of interception and catching. This chapter describes a simple multimodal system conceived for a direct application in the clinical practice for investigating and measuring human performance. The complex 3-D task of catching a ball has been simplified to a planar task where the ball is replaced by a moving object on a linear slider, in order to eliminate the influence of the gravitational model already learnt by the CNS. The system could be particularly useful for investigation in motor planning and organization, through the integrated (kinematic, dynamic, neural) analysis of the time instants preceding the actual movement.

Basic components of the platform are described and their application to human subjects is presented. In particular preliminary experiments on young healthy people of motion analysis (in terms of kinematics and dynamometric measures) and EEG measures are reported.

3.1 Rationale

In studies on human motor control, a specific task is often selected in order to investigate the mechanism of tuning motor behavior according to the perceived sensory information and cognitive representation [141, 142, 143, 144]. For instance, catching a moving ball is a natural and ordinary task cited in the literature to study preparation to tuning motor behavior [144, 145, 146, 147, 148]. It appears particularly attractive for neuroscientific investigations as it requires coordinating several limb muscles acting on different limb joints within rigid spatio-temporal constraints, due to the necessity of intercepting the moving ball. Studying how a catching task is performed offers a wide scenario of research topics ranging from limb kinematics analysis (e.g. correct positioning in defined spatio-temporal constraints) and limb dynamics, up to motor prediction, generation of internal models in the CNS, and also compliance control during catching, particularly in the interaction with the ball [149]. Prediction of impact parameters, basically based on visual information and cognitive interference, is regarded as a key factor of interception and compliance adjustment. In [145, 151, 150], for example, anticipatory and reflex behaviours associated with catching in presence of vision are extensively investigated.

In this work, the task of catching a moving object is regarded as a natural and ordinary task which allows investigating human performance of motor control following a disease or a trauma and thus eligible for functional assessment of injured people in clinical practice. The attention of this analysis was devoted on the instants just before the initiation of the actual movements, to investigate the activation of motor areas, more generally, on motor planning.

3.2 The catching platform

A mechatronic platform (henceforth named the “catching platform”) has been designed for the controlled release of the object to be grasped, in order to make the task controllable and repeatable and allow recording and monitoring human gestures and kinematic and dynamic parameters during motion. The system is specifically arranged to provide clinicians with a tool for assessment able to ensure task repeatability, affordance, reliability and simplicity of data interpretation; also, a further requirement of producing a low-cost system with respect to the other more complex technological devices [152, 153, 154, 100] used in the literature for the same purposes has been taken into account. The catching platform has a modular structure which allows gradually increasing



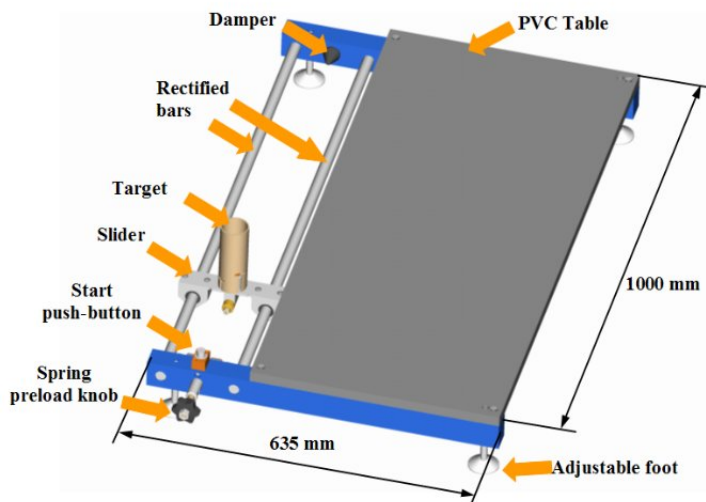


Figure 3.1: Design and description of the catching platform

the complexity and the cost of the system and, on the other hand, allows purposely reconfiguring the system to address different issues, from the single motion analysis up to the multimodal analysis of signals from different sources (for example motion signals and neurophysiological signals). This permits to bring improvements to each module independently from the others and, in a future perspective, makes the system reconfigurable also for experiments of neuroscience for investigating catching-related issues, such as human strategies for interception, the role of gaze in the interception, the issue of velocity matching between the hand and the target, the regulation of arm impedance during the motion task, etc. The design and the arrangement of the catching platform for functional assessment of healthy and injured people, in view of an application to clinics, is described. Analysis on healthy people is mainly addressed to extract performance indexes to be used as benchmark for patients. The platform is made of a basic catching apparatus for the controlled release of the object and a specific sensory system that is changed according to the issue to investigate and the parameters to measure.

The catching apparatus is a planar device with a linear slider which constrains the object to a straight-line motion. The complex 3-D task of catching

Giuseppe Cavallo

a ball [145, 150] has been simplified into a planar task where the ball is replaced by a moving object on the linear slider. In this way the influence of the gravitational model already learnt by the CNS is eliminated. The customized sensory and acquisition systems have a common purpose of providing information on the force and the kinematic parameters applied during the task. However, the type, the number and the location of the sensors is strictly dependent on the investigation addressed, the phenomena to analyse and, also, the required complexity and cost of the system. The next section provides a detailed description of the basic components of the mechatronic catching platform and demonstrates the feasibility of reconfiguring the sensory system based on the parameters to measure and the addressed analysis. Still remaining in the scenario of systems for functional assessment, in the following sections the application of the catching platform to multimodal motion and neurological analysis is presented with preliminary results.

The simplicity of the mechanical system and the modularity of the platform allow integrating acquisition systems for motion analysis with neurophysiological acquisition systems and extend human behavior analysis to neurological aspects related to reorganization and modification of cortical areas following rehabilitation therapy. To this regard, the use of the mechatronic platform with brain analysis technologies (like EEG) and muscular activity monitoring systems (e.g. EMG) is proposed in addition to acquisition systems for kinematics and dynamic parameters.

3.2.1 Design of the catching apparatus

The design of the catching platform tries to address the following two main issues:

- to remove the contribution of gravity on the object motion;
- to easily vary the momentum applied to the moving object.

The first issue implies a simplification of the catching task into a planar task. The second issue entails the possibility of selecting different motion conditions for the object to be used in studying different topics. In view of that, a straight linear motion for the target object is chosen and a spring pushing system to release the object by varying the momentum is designed. The catching apparatus is shown in Fig.3.1. It consists of a linear slider moving on two rectified bars, provided with two low friction linear bearings to ensure minimum slider velocity loss during motion. A cylindrical interface for the target

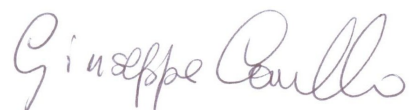
Giuseppe Cavallo

assembling is located on the slider. The interface allows positioning different objects and sensors depending on the issue addressed. The PVC 1000×450 mm table is used as reference plane for the planar motion and is supported by two square aluminum bars. On the left aluminum bar the slider push system is placed. It supplies the impulse for the slider. The push system is based on spring preloading that allows varying the momentum transmitted to the slider: the target moving object can be caught at different speeds depending on spring preload. A button on the top of the bar actuates the release mechanism that, when pushed, let the target object move immediately. The system is designed to reach a slider velocity up to 2 m/s and the available stroke is 900 mm. On the right bar a rubber shock-absorber is placed in order to adsorb slider kinetic energy.

The setup is propped by four adjustable supports which allow varying the height and the orientation of the reference plane. In this way the height of the table can be adjusted according to the anthropometric dimensions of the subject; on the other hand, by varying table orientation is possible to vary the gravity contribution to the slider motion. The moving object mounted on the catching apparatus is a 50 mm diameter aluminum tube. The diameter is chosen according to 95th percentile of the grip circumference, as reported in [125]. Finally, an array of Hall effect sensors is located on the edge of the PVC table in parallel to the direction of the slider motion, which is used to compute the target average velocity.

3.2.2 The sensory system

An ad hoc sensory system has been integrated with the catching apparatus in order to provide motion information before catching the moving object as well as during interception. The sensory system is basically composed of i) a force module for dynamometric measures during interception; ii) a magneto-inertial module for measuring limb kinematics parameters during the execution of the motor task (before and during interception). The module for dynamometric measures consists of a force sensor mounted at the base of the cylindrical moving object (Fig.3.2.a). The force sensor is a JR3 6-axis load cell having a diameter of 50 mm and a thickness of 31 mm. It allows measuring forces belonging to the range of $[-150, +150]$ N. The magneto-inertial module is the commercial unit *Xsens MTx* (Fig.3.2.b), which integrates one tri-axial magnetometer (3D compass), one tri-axial accelerometer and one tri-axial gyroscope for 3D measures. It provides in output roll, pitch and yaw orientation angles (calculated by an embedded processor), the 3D linear acceleration, the rate of



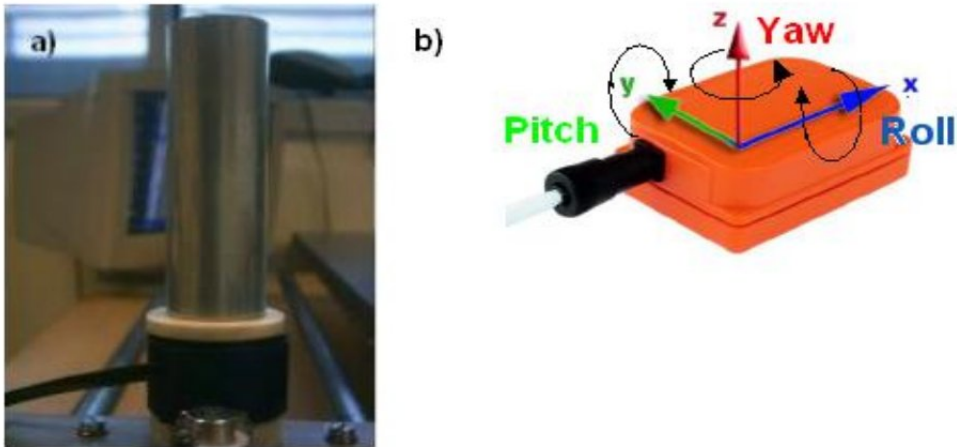


Figure 3.2: (a) The moving handle with the JR3 load cell beneath. (b) The magneto-inertial sensor (Xsense)

turn (gyro) and the earth magnetic field (in absence of other magnetic fields). The module is easily wearable since it has dimensions of $53 \times 38 \times 21 \text{ mm}$ (WxLxH) and weight of 30 g , small enough to be placed on human body segments. Data from sensors are gathered and processed in real time in order to reconstruct the 3D orientation of the module by means of a sensor fusion algorithm. The calculated orientation has a static accuracy of about 0.5° and a dynamic accuracy of about 1.0° . Accelerometers have an accuracy of about $\pm 1 \text{ mg}$ with a 95% confidence level.

Also, a specific calibration procedure can be used in order to compensate for possible distortions due to the interaction between the magnetic field and ferromagnetic objects. The gyroscopes, the accelerometers and the magnetometers present a full scale value compatible with healthy human average performance [156] of $\pm 300^\circ/s$, 1.7 g (being $g = 9.81 \text{ m/s}^2$ the gravitational acceleration) and $\pm 750 \text{ mGauss}$ (compatible with the earth magnetic field), respectively. The force and the magneto-inertial modules used with the catching apparatus are shown in Fig.3.2. The magneto-inertial module is embedded in a velcro bracelet in order to be worn by the subject during the experimental trials. When positioned at the level of styloid processes of radius and ulna, the device on the

Giuseppe Cavallo

bracelet provides global wrist acceleration (including gravity) with respect to the device reference frame and its orientation (in terms of rotation matrix) with respect to a fixed reference frame, defined during sensor initialization. The rotation matrix allows calculating the gravity contribution to be subtracted to the global wrist acceleration. Thus, an estimate of wrist velocity and position is extracted from the calculated wrist acceleration at the time interval of impact with the moving object. Numerical integration via the trapezoidal method is used to calculate wrist velocity and position and the linear drift due to integration is compensated, assuming that initial and final velocity values of the catching movements are null. Note that the magneto-inertial module can be located on any other anatomical site for position tracking purposes, by just manufacturing an ad-hoc lodgment.

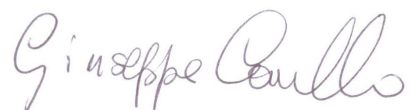
3.3 Applications of the catching platform

In this section an example of application of the catching platform to motion analysis is presented. However it is worth to stress that the modularity of the system allows the same catching apparatus to be reconfigured in order to address different scientific topics, just changing or re-adapting the sensing system and the experimental protocol to the purposes of the performance analysis and the level of complexity.

The aim of the study consists in the neurophysiological assessment of voluntary motor task. In particular the task is to catch with the upper limb a fast moving (dynamic catching) or a still (static catching) object on a plane. The attention is focused on the combined study of the neurophysiological features of sensory-motor areas and kinematic indices of movement. In particular, the aim is to characterize the cortical activation pattern through the analysis of EEG signals derived from sensory-motor areas and to correlate them with kinematic behavioural parameters.

The EEG analysis has been performed in the time instants coming before the initiation of the movement (up to 500 *ms* earlier) to analyze cortical circuit devoted to voluntary movement organization and planning. The EEG analysis was limited only to those intervals because of the presence of artifacts in the EEG tracks due to the fast movement. The EEG device (*Brain Amp*) is able to capture up to 32 EEG channel in parallel with a sample frequency of 256 *Hz*.

One channel of the system is used as an input trigger: it is connected to a series of resistors, so that when the handle is at the rest position, the electric circuit is shorted and the trigger channel reads 0 *V*, while as the handle



starts, the trigger channel detects a small voltage (few mV). In this way the exact instant when the handle leaves is detected by EEG system allowing data synchronization with the other sensors.

This is a functional study that could be considered as a starting point and an essential introduction for other type of analysis:

- the study of the performances and behavioural strategies adjustments in complex motor tasks for elderly people
- the assessment of motor impaired patients and the identification of possible prognostic markers for the achievement of the best recovery process
- the assessment of patients with movement impairment (i.e. Parkinson) and the study of the adjustment of their motor strategies

3.3.1 Motion analysis and experimental protocol

The acquisition of arm kinematics data during the catching task is a fundamental step to measure motion parameters and to study synergies and strategies adopted by human subjects to successfully perform the motion task. Here, arm motion is analyzed by means of the magneto-inertial wearable device of the sensory system described previously. It provides information about arm kinematics during the motion task, even if the numerical integration needed to extract limb velocity and position implies some issues. The data acquired by the motion capture system are transmitted to a PC serially through a USB interface. The experimental protocol for motion acquisition is explained in the following. The subject is sat on a chair in front of a table. The catching apparatus is placed on the table and the PVC support is regulated at middle sternum height. The subject is constrained to the chair by belts to avoid trunk rotation during catching movements and the chair is positioned so that the subject chest is about 50 mm far from the PVC table edge. Further, the sagittal plane of the subject has to be aligned with the middle axis of the PVC table. The subject has the hand closed and the right forearm leant on the PVC table. The start position is within the $70 \times 100\text{ mm}$ rectangular area traced on the table surface and the 5th metacarpal head has to be aligned with the distal line of the start position area. The left arm is leant on the left leg. Starting from the initial rest position, the subject has to intercept the slider and grasp the target object that is released without any warning. Movement is planar, with the forearm parallel to the PVC surface.



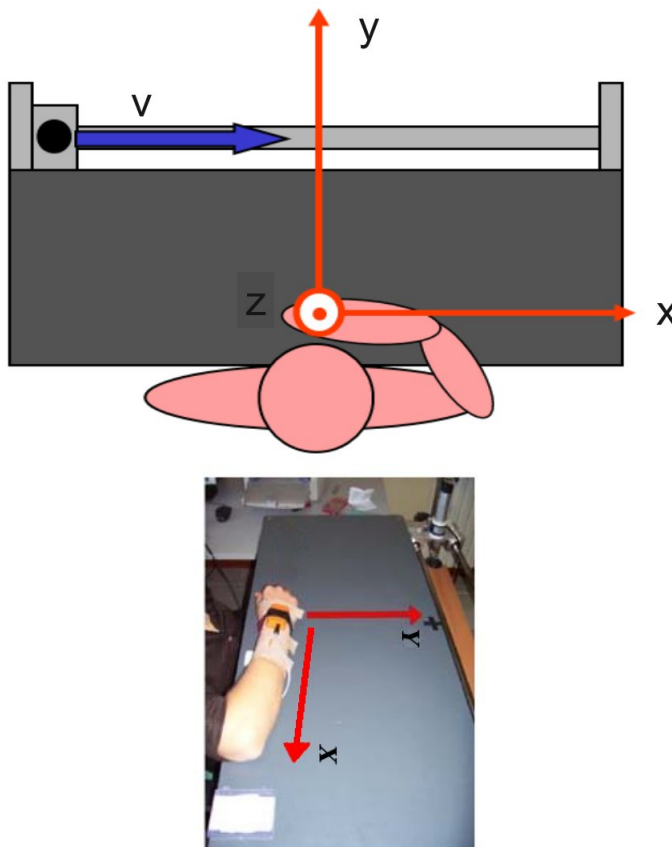


Figure 3.3: Schema and picture of the experimental setup and the reference frame

3.4 Experimental trials and preliminary results

Catching experimental trials for motion analysis have been carried out on 10 healthy young subjects (7 males, 3 females) with an average age of 24 (ranging from 20 to 26). All subjects were right-handed.

In a typical dynamic test, the subject sits in front of the platform keeping his arm folded with his wrist near his chest. Just few instants before the handle

Giuseppe Cavallo

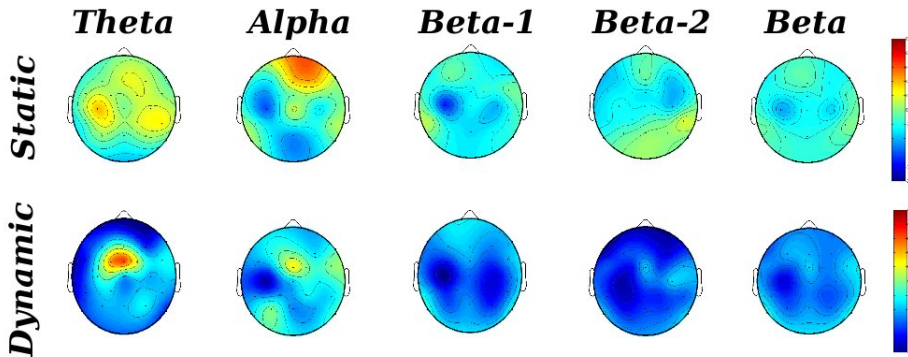


Figure 3.4: Distribution - average on all subjects - of desynchronization (ERD) and synchronization (ERS) in different bands in static catching and dynamic catching. The color blue represents the intensity of the desynchronization, while the red one represents synchronization.

starts, the subject is asked to pay attention to it; then the handle is released and he/she has to catch it as soon as he/she can. A single test lasts about 15 seconds. The time between two tests is more 12 seconds; during this period the subject is asked to relax; in this way cerebral rythm is allowed to return to the basal condition. The test is repeated for 40 times.

In the static test instead, the subject must execute the same task, at the same conditions, but this time the handle doesn't move, but it's still in the middle of the platform. So the subject is asked to catch it as fast as he can. Also in this case the test is repeated 40 times.

EEG data were elaborated through mathematical and statistical techniques (i.e. ERS/ERD and others) to derive information about the neuronal activation intensity and the position where the signals derive from. In this way it is possible to explore the cortical activation areas involved in both dynamic and static tasks in terms of synchronization or desynchronization of the signal; synchronization corresponds to an increased number of neurons firing at a particular frequency (thus impling an activation/elaboration of a specific area in a specific time) respect to a base condition; desynchronization implies the opposite.

Fig.3.4 summarizes the results obtained. The different EEG frequency

Giuseppe Cavallo

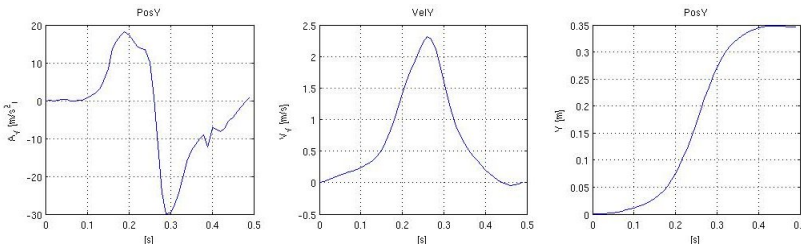


Figure 3.5: From left to right, acceleration detected by the magneto-inertial sensor and velocity and position extracted from acceleration. In particular the y-component is shown

bands are reported horizontally, while vertically there are the two different tasks (dynamic and static). Different behaviours can be noticed in the two cases, static or dynamic catching. Data on alpha and beta bands (which are used in literature for movements evaluation) confirm what reported in literature about a generalized desynchronization taking place during pre-movement phase. Theta band which is related with sensorimotor integration and planning during complex tasks, is much more desynchronized in the dynamic task rather than in the static. This result could be explained assuming that human brain consider the static task much simpler than the dynamic.

Concerning results on kinematic data, it should be noticed that the mathematical technique deriving positions and velocities from accelerations provide only an estimate of them, because of the error drift affecting the acceleration signal. However a acceptable results can be obtained compensating the drift numerically by assuming that it is constant along time. This assumption can be considered reliable within small intervals of time (i.e. a catching movement) as the error in position increases as the square power of the time.

So to perform a correct extraction of position and velocity, some constraints are needed: first of all the initial and the final velocity of the movement must be zero. This condition allows to force the initial and the final point of the velocity vector to be zero, thus eliminating the eventual linear drift error. Finally, as already mentioned, the task should be as shorter as possible. The shorter the signal, the more reliable position and velocity are.

Fig.3.5 shows a typical acceleration, velocity and position profile. They confirm data present in literature about minimum jerk theory of voluntary movement with the typical bell shape, [159], [154]. Fig.3.6 presents the recon-

Giuseppe Cavallo

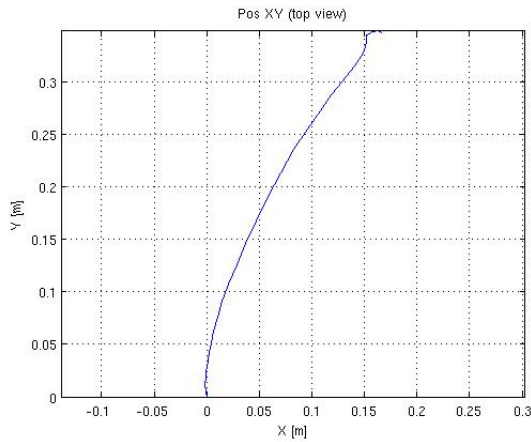


Figure 3.6: Reconstruction of the trajectory followed by subject's wrist (top view)

structed x-y position of the subject's wrist movement on the platform plane. The rest position is in $(0, 0)$, while the sliding handle should be imagined horizontally at the top of the graph (at about $30 - 35$ cm).

Different kinematic and dynamic features have been extracted from these signals to obtain indices of motor performance. The following list illustrates the most meaningful of them:

Contact Time Time between handle starting and the instant of interception

Time to Contact (TTC) Time between acceleration peak and instant of catching; the use of this parameter was inspired by a previous work [161]

Interception position X and Y position at the instant of interception respect to the wrist rest position (before the task initiation)

Max velocity Peak in the velocity curve (bell-shaped)

Interception force Value of force at the instant of interception

A preliminary analysis of these result shows a general trend towards an improvement of performances in most subjects as the number of tests increase. In particular it has been noted that for 8 subjects there are statistical difference

Giuseppe Cavallo

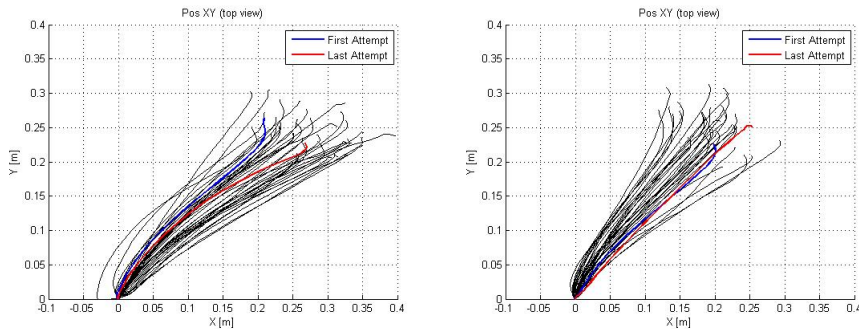


Figure 3.7: The left plot shows the first 20 tracks (top view) extracted from subject's wrist acceleration signal, the right plot shows the other 20. The starting point was fixed at the axis origin. Trajectories endpoints are moves towards the rest position of the handle as the subject learns the task

($p < 0.05$) for most of the indices between the first 20 trials and the last 20 in the dynamic task. This could be explained in terms of motor learning, assuming that the subject continuously keeps on learning how to correctly execute the task and improving his performance during the experimental tests. As the subject learns, interception position moves left towards the rest position of the handle, the interception time, the TTC, the maximum speed and the maximum force decrease. Fig.3.7 shows at a glance the improvement of the performance (in particular the shift of the interception position along y-axis) of a subject.

3.5 Conclusions

A new mechatronic platform has been presented for studying motor control performance of human subjects during an ordinary task of catching a moving object on a plane. A preliminary experimental validation of the platform for measuring human performance has been carried out, in order to study and demonstrate its applicability to functional assessment of injured people with respect to healthy subjects. Also a demonstration is provided of how the system can be reconfigured to investigate and measure different parameters with different levels of hardware complexity and costs. The platform mechatronic components have been described in detail and their potential use in studies of motion analysis have been presented. For the first application of motion

Giuseppe Cavallo

analysis, the catching apparatus has been equipped with two different sensory systems for measuring motion kinematic and dynamic parameters (the Xsens MTx module and the JR3 load cell) and the experimental results on limb trajectory and velocity have been reported. The Xsens MTx module embedded in a wearable bracelet has been also jointly used with a module of force measure for estimating limb impedance. The experimental protocol and the preliminary results on static impedance measure have been reported. EEG results confirm what reported in literature about movement planning and cortical activation before the movement initiation and show the major complexity of the dynamic task respect to the static one perceived by the brain (desynchronization in theta band). Kinematic and dynamic analysis highlight instead an improvement in motor performances as the number of tests increase. This preliminary result, if furtherly confirmed, could be explained in terms of motor learning and could provide a useful parameter for clinical or research assessment of motor learning capabilities of a subject.

Giuseppe Cavallo

Chapter 4

Neurodevelopmental Engineering

This chapter offers a first sight towards a new promising discipline called Neurodevelopmental Engineering. It mainly aims at quantitative analysis and modeling of human behaviour during neural development to understand or discover the causes of behavioural disorders (such as the Autism). This new research area is deeply multi-disciplinary, so that also Mechatronics can give its contribution to this purpose by providing innovative ecologic and unobtrusive tools, so not to alter (directly or indirectly) the natural behaviour of the tester.

Following these criteria, the whole experimental setup must not require any structured environment; this implies a series of issues to be faced and in particular the problem of tools calibration which generally is performed in structured metrologic labs and requires very high quality instrumentation.

A first example addressing this problem is illustrated in this chapter, presenting a new technique for in-situ calibration of magneto-inertial orientation sensors for motion tracking and orientation analysis in children.

4.1 Introduction

Neurodevelopmental engineering is a new interdisciplinary research area at the intersection of developmental neuroscience and biomedical engineering aiming at providing new methods and tools for:

- (i) understanding neurobiological mechanisms of human brain development
- (ii) quantitative analysis and modeling of human behaviour during neural development

- (iii) assessment of neurodevelopmental milestones achieved by humans from birth onwards
- (iv) studying neurodevelopmental disorders
- (v) conceiving new telematic, mechatronic and robotic components and systems for applications on infants and toddlers, which can be used also in ecological conditions for long periods of time
- (vi) investigating ethical, epistemological and social implications related to this research activity.

The approach proposed by Neurodevelopmental Engineering allows, as example, the development of novel methods and devices to evaluate basic patterns of goal-directed actions in normally developing babies, under naturalistic conditions. The quantification of behavioural data in normal children could establish standards against which development of infants at risk for neurodevelopmental disorders, particularly autism spectrum disorders (ASD), can be measured, with the aim of detecting early signs of disturbed development.

In order to assess infants neuro-development, it could be useful monitoring some particular aspects of children behaviour such as:

- Basic sensorimotor integration/patterns of gaze
- Expression of emotions
- Social communication

4.2 Autism as neurodevelopmental disorder

Autism is a behavioral disorder, with onset in childhood, which is characterized by deficits in three basic domains: social interaction, language and communication and pattern of interests. There is no doubt that autism has a strong genetic component, and that biological disease mechanisms leading to autism are already active during fetal development and/or infancy. Autism is typically diagnosed at the age of 3 years and not earlier than 18 months [74]. The diagnosis of autism is purely clinical, there are no laboratory tests to confirm or disprove the diagnosis. Current assessment protocols of ASD are based, among other items, on the observation of the child while playing with toys or on pretend play [74, 75]. As a matter of fact, the only attempts at an early diagnosis of autism have been made by rating of home videotapes of behavior from very



young children later diagnosed with autism [76, 77]. This qualitative approach proved very useful in laying down the bases for research in this field, but at the same time urges for novel quantitative approaches and enabling technologies.

4.3 Tools for early diagnosis

The most advanced technological set-ups available in research labs on autism/developmental disorders may currently include some sophisticated systems for movement analysis, such as:

Stereophotogrammetric systems for movement analysis. These are rather sophisticated and costly technologies. They require highly structured environments, and generally cameras have to be carefully positioned and calibrated.

Gaze-tracking devices the systems so far in use, including commercially available ones, can be applied in specific contexts. Generally, the subject is required to face specific directions, e.g., they are particularly suitable when the subject looks at a TV screen. Gaze-tracking devices become unsuitable in the case of infants.

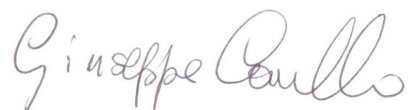
Force platforms often combined with photogrammetric systems, they are used to measure ground reaction forces (GRFs) as the subject walks on the platform. A major limitation is that measures are provided only when the subject steps on the platform, i.e., they are not continual.

Data gloves only recently have some research projects faced the problem of developing data gloves for the child, which can be potentially combined with customized virtual reality environments.

A limitation common to all previously mentioned technologies is that, despite providing very accurate measurements, for the extracted data to make sense, tasks need to be performed in well-controlled and highly structured environments as well as in accurately known and repeatable conditions.

Aiming at not to alter the natural behaviour of the child when analyzed, technologies for the domain of neurodevelopmental engineering should respond to the following main requirements [28]:

Non-obtrusive technology: the new devices should be designed with the final goal of continual monitoring, but without being distressful to the



child. In fact, the child should either not perceive the presence of such instruments at all (e.g., wearable microphones, cameras, etc.) or like to play with them (e.g., instrumented toys). This clearly sets constraints on the kind of technology to be used. In particular, small size, light weight, wireless and portable will be the key features to take into account during the technical design of such devices.

Minimally structured operating environments: current tools for behavioral analysis, e.g., photogrammetric devices for motion analysis or force platforms for gait analysis or state-of-the-art gaze-tracking devices, are only suitable for controlled and highly structured environments such as research laboratories. Screening of a large number of children for diagnostic purposes is therefore not feasible due to high costs and limited availability of the equipment. The best choice would be the development of relatively low-cost devices requiring minimally structured environments. Possible settings range from totally unstructured home-like situations, e.g., the child plays with interactive toys while a caregiver steers the game along predefined play protocols and tasks, to situations with an increasing degree of structuring.

4.4 The calibration issue

Those considerations must be seen as technological constraints to deal with when developing new devices for behavioural analysis. Behavior monitoring includes, for example, tracking a child's posture, tracking the head direction (which mainly relates to the child's attention), tracking position and/or orientation of toys while the child plays with them, etc...

Mechatronic devices developed for this purpose must be deployed to be embedded in a child's everyday environment, e.g. in toys and clothes. For this reason special attention must be paid to technologies which do not require costly equipment (e.g. photogrammetric systems) and/or a structured environment (e.g. motion analysis laboratories). The technology of interest should be able to work in clinical settings as well as at home and should be operated by minimally trained personnel, e.g. the child's caregiver. Specific care should be devoted to sensors calibration: infact this procedure, absolutely necessary to measurement reliability, is time-consuming and often requires the use of an ad-hoc expensive and high quality instrumentation and/or structured environment.



In this sense, orientation tracking based on inertial/magnetic sensors [79, 78, 80] represents a promising technology since, as shown in next sections, orientation of a rigid body can be measured solely relying upon gravitational and geomagnetic fields, which are present everywhere on earth, without the need of other sources of fields, i.e. sourceless. Furthermore accelerometers and magnetometers are nowadays available in packages small enough to be worn or embedded into toys and can be used to track position/orientation in unstructured environments.

Many commercially available devices allow on-board calibration by means of addition of external circuitry, mainly used to generate artificial fields which act on the sensor itself as a known forcing input. Addition of external circuits is a major drawback in applications such as the one of interest, where the technology has to be worn by infants.

In this work, a novel procedure for in-field calibration of magnetometric sensors is presented which does not rely on previous knowledge of magnitude and direction of the geomagnetic field and which does not require accurately predefined orientation sequences. Such a method proves especially useful in clinical applications since the clinician is no longer compelled to execute accurate calibration protocols.

4.5 The proposed solution: in-field calibration

Magneto-inertial devices are sensors integrating accelerometers (used as inclinometer), magnetometers and gyroscopes to derive the orientation of a rigid body. The redundancy of information is used to enhance the reliability of the orientation measurement through the use of complementary filters. In this application only magnetometers and accelerometers will be considered.

4.5.1 Magneto/Inertial orientation tracking

Accelerometers, in static conditions, directly provide a measure of the gravity vector g which is always vertical with respect to the earth surface. Magnetometers measure the geomagnetic field b when no other magnetic source is present. Geomagnetic field has an horizontal component b_{\parallel} which points towards *North* and a vertical component b_{\perp} which depends on the latitude. Define now a third vector:

$$\mathbf{h} \triangleq \mathbf{g} \times \mathbf{b}$$



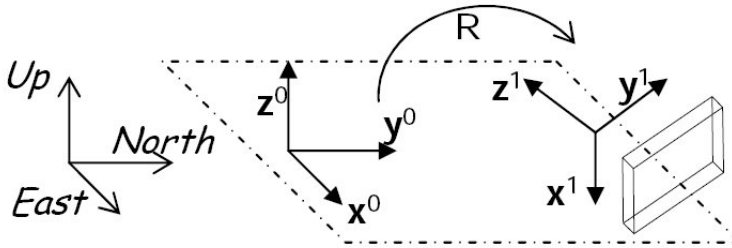


Figure 4.1: Fixed and moving coordinate frames, respectively $\{\mathbf{x}^0, \mathbf{y}^0, \mathbf{z}^0\}$ and $\{\mathbf{x}^1, \mathbf{y}^1, \mathbf{z}^1\}$

where “ \times ” is the vector product in 3D Euclidean space. It is worth noting that \mathbf{h} is never null (since \mathbf{g} and \mathbf{b} are never collinear) and always points towards *East*. The three vectors \mathbf{g} , \mathbf{b} , and \mathbf{h} are therefore independent and can be used to define a convenient fixed coordinate frame $\{\mathbf{x}^0, \mathbf{y}^0, \mathbf{z}^0\}$:

- \mathbf{z}^0 : unitary vector pointing *Up*
- \mathbf{x}^0 : unitary vector pointing *East*
- \mathbf{y}^0 : unitary vector pointing *North*

This can be expressed in invariant (i.e. valid in every coordinate system) geometrical terms:

$$\begin{aligned}\mathbf{z}^0 &\triangleq -\mathbf{g}/g \\ \mathbf{x}^0 &\triangleq \mathbf{h}/\|\mathbf{h}\| \\ \mathbf{y}^0 &\triangleq \mathbf{z}^0 \times \mathbf{x}^0 = \mathbf{h} \times \mathbf{g}/\|\mathbf{h} \times \mathbf{g}\|\end{aligned}$$

where $g = \|\mathbf{g}\| \approx 9.8 \text{ m/s}^2$.

Let now $\{\mathbf{x}^1, \mathbf{y}^1, \mathbf{z}^1\}$ be an orthonormal frame (referred to as moving frame) defined via the sensitive axes of the sensorized system (the tilted box in Fig.4.1) whose orientation should be determined with respect to the fixed frame. With reference to Fig.4.1, the fixed frame $\{\mathbf{x}^0, \mathbf{y}^0, \mathbf{z}^0\}$ and the moving frame $\{\mathbf{x}^1, \mathbf{y}^1, \mathbf{z}^1\}$ are related by a rototranslation. The translation is ignored hereafter (the origins of the two coordinate frames shall always be imagined as coincident) since

Giuseppe Cavallo

only relative orientation is of interest. It can be demonstrated [81] that because of the invariance of geomagnetic and gravitational fields, the rotational matrix can be obtained with simple algebraic manipulations from accelerometers and magnetometers' read-out.

4.5.2 The calibration procedure

This procedure for 3D orientation detection implicitly assumes that accelerometers and magnetometers provide direct measurement of the components of the gravitational fields (g_x, g_y, g_z) and of the geomagnetic field (b_x, b_y, b_z). In fact sensors are just transducers and provide an output voltage v that, in the best scenario, is proportional to variations of the measurand m . In practical terms: $v = km + v_o$, where k and v_o respectively represent the linear gain and the offset value. A calibration procedure is needed to determine such coefficients in order to derive the measurand $m = (v - v_o)/k$. Parameters v_o and k are easily determined when situations exist where the measurand assumes (at least) two known values. In the case of accelerometers, the measurand can easily assume values $0, +g$ and $-g$ by simply aligning (e.g. by means of mechanical set-ups such as a pendulum) the sensor's axis, respectively, orthogonally, parallel and anti-parallel with the vertical direction. When it comes to the magnetic field, alignment of the sensor's axis with the field's direction is not straightforward. For this reason an additional field has to be generated.

Commercially available devices such as the Honeywell HMC105X, a family of multi-axes magneto-resistive sensors, contain purposefully designed "offset straps", i.e. spirals of metallization that couple with each sensitive axis of the device producing an additional magnetic field. Such patented feature can be used for auto-calibration of the sensor. Such procedure requires addition of extra circuitry used to drive each offset strap. In applications where infants are supposed to wear such technology, reduction of components is highly desirable. For this reason a procedure which would only rely on the natural geomagnetic field distribution and that would not require any accurate alignment was investigated, as presented in the following.

The proposed procedure solely relies upon uniformity of the natural geomagnetic field. This means that components with respect to the fixed frame (i.e. $[0 \ b_{\parallel} \ b_{\perp}]^T$) are constant throughout space¹.

¹Such requirement is not too strict although some care should be taken, refer to [78] for details of usage in clinical practice



As the device is oriented in space, the moving reference attached to it (refer to Fig.4.1) is also subjected to the same orientation and the field components in the moving frame (i.e. $[b_x \ b_y \ b_z]^T$) change accordingly. As pointed out in the previous section, this change of coordinates is fully determined by the rotation matrix R . Rotations in space are linear transformations which act on vectors preserving their modules (a major property of rotation matrices):

$$b_x^2 + b_y^2 + b_z^2 = constant = b_{\parallel}^2 + b_{\perp}^2$$

This means that, as the device is being displaced and oriented in space, the geomagnetic vector is seen by the moving frame as a time-varying vector of constant module, i.e. the trajectory of its end-point (b_x, b_y, b_z) is bound to stay on a sphere centered in the origin and of radius:

$$b = \sqrt{b_{\parallel}^2 + b_{\perp}^2}$$

In terms of sensor output voltages (v_x, v_y, v_z) , considering different offset voltages (v_{ox}, v_{oy}, v_{oz}) and different linear gains (k_x, k_y, k_z) for each axis, the sphere becomes now an off-centered ellipsoid:

$$\left(\frac{v_x - v_{ox}}{k_x}\right)^2 + \left(\frac{v_y - v_{oy}}{k_y}\right)^2 + \left(\frac{v_z - v_{oz}}{k_z}\right)^2 = b^2$$

or equivalently

$$\left(\frac{v_x - v_{ox}}{bk_x}\right)^2 + \left(\frac{v_y - v_{oy}}{bk_y}\right)^2 + \left(\frac{v_z - v_{oz}}{bk_z}\right)^2 = 1$$

Such an ellipsoid is uniquely identified by the six parameters $(v_{ox}, v_{oy}, v_{oz}, bk_x, bk_y, bk_z)$, the first three identify the center of the ellipsoid, the remaining three identify the semi-axis length of the ellipsoid. At least six independent equations are needed in order to determine the unknown parameters. Such equations can be derived as part of the calibration procedure: a sequence of N orientations in space allows measuring the sensor read-outs (v_{xi}, v_{yi}, v_{zi}) relatively to each orientation $i = 1 \dots N$.

Because of the errors (measurement noise) affecting the sensor read-outs, least-squares fitting methods applied to a larger number ($N \gg 6$) of measurements can be deployed to obtain an estimate of the six unknown parameters which is less sensitive to measurement noise.

For sake of clarity, rewrite the N nonlinear equations

Giuseppe Cavallo

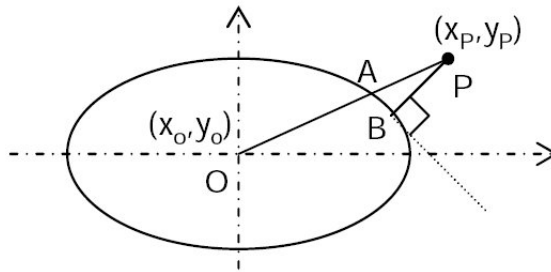


Figure 4.2: Distance of a point P from an ellipse: although BP represents the true geometrical distance, AP is used instead as an analytically convenient approximation.

$$\frac{(x_i - x_0)^2}{a^2} + \frac{(y_i - y_0)^2}{b^2} + \frac{(z_i - z_0)^2}{c^2} - 1 = 0$$

where $i = 1 \dots N$ and where obvious changes of notations (e.g. $v_{xi} \rightarrow x_i$, $v_{ox} \rightarrow x_0$, $b k_x \rightarrow a$, etc...) are made. Least-squares fitting is probably one of the most widely used approaches for estimating ellipses' parameters [82]. In general there exist no exact solution satisfying all of the N equation, what can be found is an estimate which minimizes a given error-of-fit (EOF) function ($e_i(\mathbf{p})$, where $p = [x_0 \ y_0 \ z_0 \ a \ b \ c]^T$ is the vector of 6 unknown parameters which fully determine the ellipsoid).

Several choices are possible for the EOF, see [82] for details. The purpose of an error-of-fit function is defining a sort (not necessarily positive definite) of distance of a generic point from an ellipse. With reference to Fig.4.2, for a point P of coordinates (x_p, y_p) the most intuitive choice would be the geometrical distance BP . Unfortunately for a generic point P off the ellipse, the analytical derivation of B is not so straightforward. As an analytically convenient approximation, the length of AP can be used instead, where the point A is simply where the ray OP intersects the ellipse.

Such vector \mathbf{p} will be eventually determined by numerically solving:

$$\min_p \sum_{i=1}^N e_i^2(\mathbf{p})$$

Giuseppe Cavallo

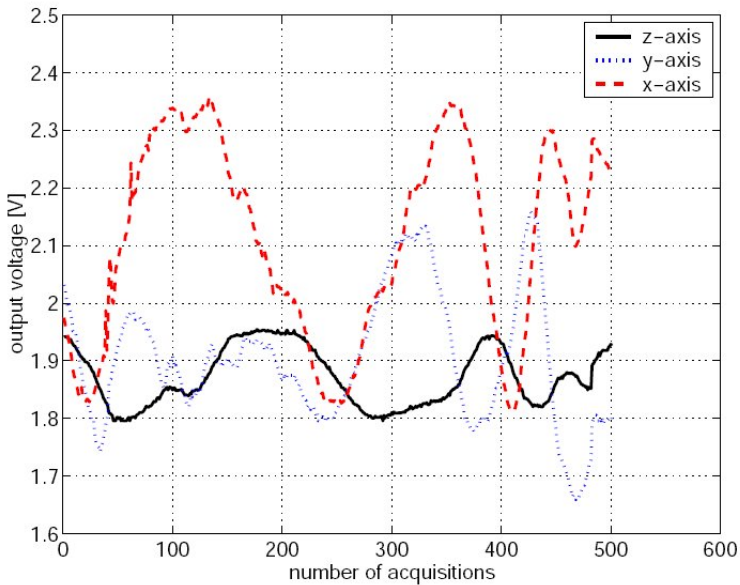


Figure 4.3: Measurement sequence: 3-axis sensor's amplified read-outs

4.5.3 Experimental setup and results

In order to validate the previously described calibration procedure, an experimental setup consisting of:

- one HMC1051: a 1-axis magnetometer sensing the field in the z-direction;
- one HMC1052: a 2-axis magnetometers sensing the field in the xy-plane;
- three amplifying stages: one for each axis;

The device was placed in a wooden box and randomly (manually) moved around in 3D space for a few seconds while amplified data were being acquired and stored on a computer for later processing. Care was taken not to simply translate the box but to provide random orientation as well. Fig.4.3 shows the experimental data as acquired voltages at the output of the three amplifying stages.

Giuseppe Cavallo

Considering the 3D space of measurements (x_i, y_i, z_i) , the sequence of N measurements appears as a cloud of points (see the left plot in Fig.4.4) distributed along the surface of the ellipsoid yet to be determined (presence of measurement noise causes these points not to perfectly lie on the surface).

In order to numerically determine the ellipsoid (i.e. its six parameters), calculations were carried out in the MATLAB environment.

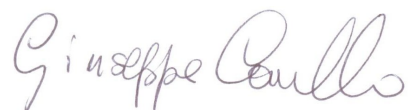
The best fitting ellipsoid, besides being off-centered due to bridge offsets, revealed different sensitivities among different axes, as illustrated in Fig.4.4. In particular, the z -axis ($c = 0.07 V$, while $a = b = 0.27 V$) is much less sensitive than the x and y axis. This is due to the fact that an HMC1051 was used to sense the field in the z -axis while an HMC1052 was used for the remaining ones. In practical situations, different devices may display different sensitivities for a variety of reasons. The proposed calibration procedure proved capable of overcoming such problems. This directly translates into a clinical protocol which requires the human operator (who, for example, wears such devices on his/her upper limbs) to perform a set of predetermined actions (lifting an arm, pointing right or left etc ...) which need to be only qualitatively described, i.e. a procedure which is more suitable to a clinical practice.

4.6 Conclusions

In this work a novel procedure for in-field calibration of inertial/magnetic wearable devices for orientation tracking was presented. Although several techniques for calibrating such devices already exist, a novel method was investigated with the specific aim of being deployed in clinical practice, where existing procedures often prove impractical and lead to disuse.

Emphasis was placed on the fact that a human operator would perform the orientation sequence needed for calibration and that such orientation sequence should be only qualitatively described, requiring no particular dexterity or performance accuracy.

A geometrical description of the problem was used to show that, although randomly generated, all the measurements were expected to lie on the surface of an ellipsoid. The least-squared fitting method was used to determine such an ellipsoid described by six parameters representing three offsets and three gains values needed for calibrating a 3-axis magnetic device (this work focused on magnetometers since accelerometers generally pose much fewer problems). Accurate calibration was finally obtained by having a large number of random orientation sequences rather than a few accurately performed ones. To this



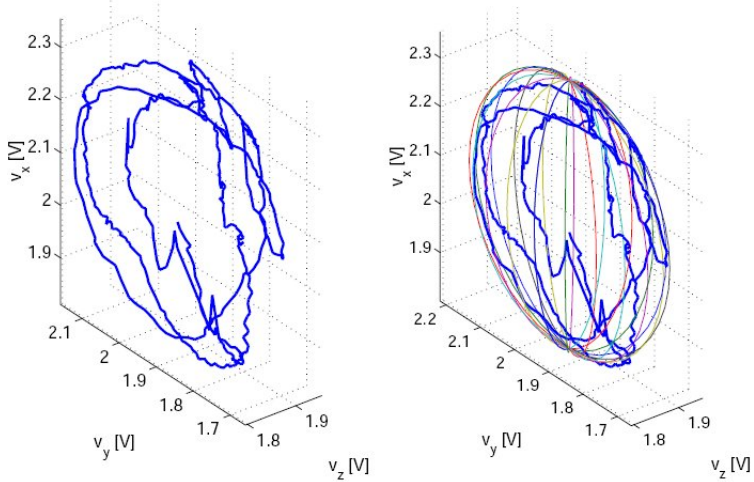


Figure 4.4: *Left*: “cloud” of measurements, i.e. the trajectory of measurement sequences in 3D space. *Right*: best fitting ellipsoid (thin lines) superimposed with cloud of measurements (thick lines).

end, the least-squares fitting approach proved essential both to exploit the large number of measurements and to gain robustness with respect to measurement noise

Giuseppe Cavallo

Chapter 5

Isometric measurements in post-stroke patients

This chapter deals about an innovative platform for whole-body force and torque measurements on healthy and pathological human subjects, e.g. post-stroke patients. The platform has been designed to allow accurate quantitative measurements in isometric conditions. The first area of application for the proposed platform was functional assessment, in terms of milestones and markers of the recovery process of post-stroke patients. Preliminary results, gathered from clinical trials in three European centres, validated the viability of the proposed platform and enlightened many interesting other possible areas of application in neurorehabilitation and basic neuroscience research on motor control.

In particular here the main attention is given to signal pre-processing (i.e. onset detection, features extraction) aiming at reducing the great amount of raw data and to detect clinically significant part of the signals.

5.1 Rationale

Neuro-rehabilitation is a field of medicine in which the therapists' experience plays a fundamental role, although sometimes it lacks of rigorous biological or scientific evidences.

Clinical techniques for patient assessment routinely rely on subjective and labour intensive techniques involving gross rating scales or the application of motor behavioural tasks using motor proficiency test batteries [83, 84, 85, 86].

CHAPTER 5. ISOMETRIC MEASUREMENTS IN POST-STROKE
PATIENTS

60

Moreover the used scales lack reliability and are unable to provide the healthcare professional with a good prediction of possible impairments and disabilities nor the healthcare provider with an estimate of the cost and outcome of the treatment [87, 88].

This is the reference frame for clinical activities in neurological rehabilitation: indeed there are many “schools of thought” and different approaches to treatment making evidence-based practice complex and difficult. The heterogeneity of studies with respect to patients, research designs, treatments, comparisons, outcome measures, and results, combined with borderline results in many of the trials, limits the specificity and value of any conclusions that can be drawn from them.

This is the new contest in which the ALLADIN platform was conceived and developed. It derives as a logical consequence from the recent findings in basic neuroscience helping the research team in the conceptualization of how best to measure these variables with a high accuracy.

The underlying hypothesis is: “*Motor images are endowed with the same properties as those of the (corresponding) motor representations and therefore have the same functional relationship to the imagined or represented movement and the same causal role in the generation of this movement*”. [102]

The fact that the human brain shows important activity during the simulation of motor actions without physically executing them is important. This means that there is a neuro-psychological relationship between imaging and performing a movement or, that the mental simulation of an action correlates to a subliminal activation of the motor system.

Since, in the first days after stroke, the amplitude of each possible movement is very limited, the idea was developed to use isometric analysis at the start of a functional directed movement. The latter, in combination with movement imagination, is the ideal combination to verify the integrity of a still existing or altered “forward model¹” for a particular functional task.

The basic assumption inspiring this research work, is that the initiation of a task has the same functional properties as performing the task [106, 107, 110, 111].

Six degrees of freedom force torque measurements at the start of each functional task can shed light on the development of new correct or aberrant movement pathways towards functional objects. The start/hold component of the isometric measurement implies not only the analysis of some remaining feed-

¹ The forward model is defined as the internal representation of the causal relationship between sensorimotor signals and motor commands ([93, 94, 95]).



back control capabilities after stroke but also the discovery of any restoration activity in future predictive control loops. The latter is the optimum requirement for human functional behavior.

The ALLADIN approach for assessing the recovery state of stroke patients relies on repeated measurements of motor efforts during movement initiations for specific tasks. As the emphasis in stroke rehabilitation is on the improvement of functional performance, an ideal measuring tool must use Activities of Daily Living (ADL) tasks ([116, 117, 118, 119]) as a principle for its quantitative measurements.

5.2 The ALLADIN platform

The ALLADIN diagnostic device (fig.5.2) is capable of measuring isometric F/T trajectories during the imagination and initiation of the selected ADL tasks. It should be noticed that *no actual movement is expected by the interaction between the platform and the patients*. Stroke patients have been invited to perform six different ADL tasks in a prescribed order. The isometric F/T patterns have been simultaneously measured by 6-axis F/T sensors at 8 different body segments during the imagination and initiation of each ADL task. The main objective of the isometric F/T measurements is to obtain quantitative evidence for recovery from stroke during rehabilitation.

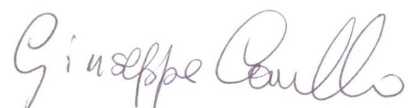
Every isometric measurement is used to determine the actual status of the patient. Therefore, it was necessary to measure a large number of patients with the same device and in the same anatomical starting position. This assures an high reproducibility during the entire period of data acquisition in clinical trials. The following two tables indicate the positions of the sensors on the patient's body and the ADL tasks to be performed.

The complete description of the ADD, the tasks to be performed and the measurement method are explained in previous papers ([133], [134], [135]).

In following sections the main focus will be on two particular aspects of the development of the platform such as:

the data pre-processing with the aim of extracting clinically relevant information from the recorded force-torque signals i.e. innovative markers and milestones of the patient recovery process

the onset detection and the identification of a time windows of interest within which to extract the the features previously identified



CHAPTER 5. ISOMETRIC MEASUREMENTS IN POST-STROKE
PATIENTS

62

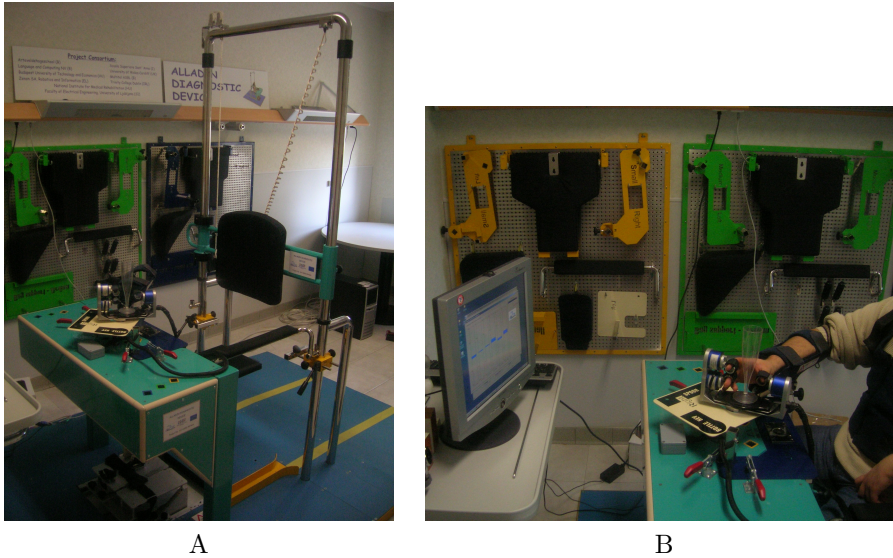


Figure 5.1: A. The ADD platform installed at Campus Bio-Medico University in Rome: 8 force/torque sensors distributed in 8 body districts allow isometric measurements on Activity of Day Living tasks in post-stroke patients. B. A detail of the orthosis for the assessment of manipulation tasks.

1	Trunk (patient's back)
2	Lower trunk (at the patient's fundament)
3	Impaired foot
4	Impaired toe
5	Impaired lower arm
6	Impaired thumb finger
7	Impaired index finger
8	Impaired middle finger

Table 5.1: Position of ADD F/T sensors on patient's body

Giuseppe Cavallo

1	Drinking a glass (no reaching)
2	Turning a key
3	Taking a spoon
4	Lifting a bag
5	Reaching for a bottle
6	Bringing the bottle to the other side

Table 5.2: Activity of Daily Living tasks to be performed by the patient

This two steps will provide an outcome to be further elaborated by a data-mining tool to derive long-term prognostic indexes that are currently missing in the clinical practice.

5.2.1 The data collected

The patients involved were recruited by the three clinical partners, resided in three different European countries. The first 8 weeks of the clinical trial patients were measured twice a week, from then on only once a week during the remaining 4 months. The main criteria for inclusion were:

1. diagnosis of ischemic brain damage
2. an obvious motor deficit
3. sufficient co-operation to permit full clinical examination

Patients with a pre-stroke disability interfering with the goal of the study were not included. A control group of healthy subjects, measured once for all ADL tasks was added to the database. They will be referred to as the Normal Controls.

5.3 The approach and the proposed solution

The final goal of the work is to have a clinical tool to assess the recovery state of a patient by detecting significant events in the recovery course, or at least to provide the clinicians with valuable information to support their diagnostic (e.g., does the patient demonstrate continuous progress or get stalled in some state, can we predict an oncoming significant recovery within a reasonable amount of time?).



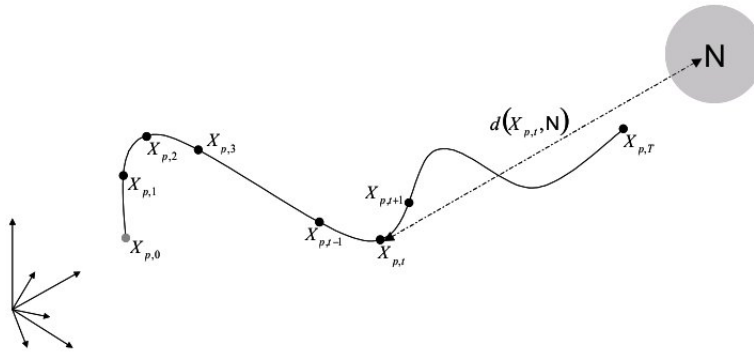


Figure 5.2: Recovery space paradigm: the stroke patient is represented by a feature vector that ideally evolves over time from his initial state to normality (N).

The adopted approach assumes that the state of a stroke patient at a given instant is sufficiently characterized by a set of features, a so-called feature vector, which is extracted from the current isometric torque/force measurements. The feature vectors evolve in a multivariate space, referenced as the Recovery Space (see 5.2). $X_{p,t}$ is defined as the feature vector computed for the p -th stroke patient and at the t -th day after the patient stroke, and this for several ADL tasks. Note that the measurement sessions are regularly spaced: every patient has two recording sessions during the first 8 weeks and 1 recording session per week for the consecutive 16 weeks. The time course of the feature vectors of a stroke patient is expected to depict the evolution of the patient from a 'diseased' towards a normal state. The direct observation of relevant patterns in sequences of feature vectors in the recovery space is untraceable because of the high dimension of these feature vectors (up to 6 dimensions in this study). The proposed approach consists in defining a measure of how far feature vectors stand from normality. Normality is meant as the population of feature vectors obtained for normal controls for the same ADL task. The expected result is that these measures of distance to normality will allow characterizing the evolution of the stroke patient in the recovery space from a more easily interpretable perspective.

Giuseppe Cavallo

5.3.1 Features definition

In a first step a large quantity of possible useful features were defined. Then through a statistical analysis a smaller subset of them selected the features mostly related to the recovery condition of the patient. Here some general criteria followed in the features definition.

In particular the defined features don't explicitly depend on the energy of the signal and the reaction time given the fact that patients neither were asked to react with maximal force neither to start as fast as possible after the start signal.

The first category of features is based on scientific researches that demonstrated that stroke patients have a typically reduced ability of controlling force/torques generation, both in intensity and spatial direction. This lack of control should somehow be reflected in a set of "abnormalities" in the force/torque vector direction. Most of them are not extracted directly from the force/torque trajectories but from the following derived variables and grouped accordingly:

- Mean effort
- Angular deviation to the mean direction.
- First-order angular deviation of the effort series.
- Cumulative sum of the effort series.

A second category of features are expected to capture other characteristics of the movement dynamics (i.e.: the rise time). These are directly extracted from the effort time series.

Another category of features was defined to catch the cross-sensor information. The definition relies on the hypothesis that the sequence of activation of the different sensors and the relative time delays during the execution of the same task can be of clinical interest for estimating 'distance to normality'. It is expected that stroke patients will demonstrate abnormal time activation patterns due to some loss of internal models of the tasks to be performed. These internal models in the brain deal with motion planning, prediction and execution. They are tightly tied to the *Mutual Information*.

Here a brief description of the parameters follow:



Mean effort direction

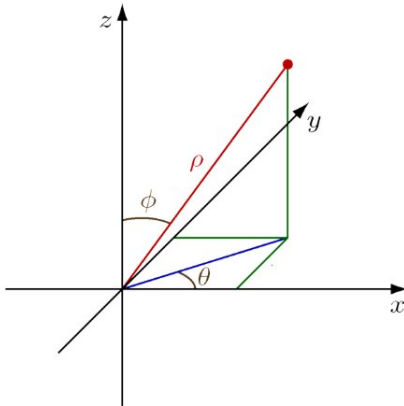
It is assumed that effort direction is more relevant for indicating recovery than pure force intensity. For example spasticity (involuntary muscle contraction) can be a source of intense force, though not functional for reaching to an object. Given a recording, for the s -th sensor, we compute the mean force direction features as the colatitude and azimuth angles of the mean force vector with respect to its referential. The mean force vector is defined by its components $\bar{F}_{s,x}$, $\bar{F}_{s,y}$ and $\bar{F}_{s,z}$ where

$$\bar{F}_{s,x} = \frac{1}{N} \sum_{k=k_0}^{k_0+N-1} F_{s,x}[k]$$

$$\bar{F}_{s,y} = \frac{1}{N} \sum_{k=k_0}^{k_0+N-1} F_{s,y}[k]$$

$$\bar{F}_{s,z} = \frac{1}{N} \sum_{k=k_0}^{k_0+N-1} F_{s,z}[k]$$

with k_0 being the sample index of the estimated onset time. The colatitude $\phi_{F,s}$ is the angle between the z -axis of the mean force vector. The azimuth $\theta_{F,s}$ is the angle between the positive x -axis and the line from the origin to the end of the mean force vector projected onto the xy -plane. These angles are obtained by converting the Cartesian coordinates of the mean force to spherical coordinates, that is,



$$\rho = \sqrt{F_{s,x}^2 + F_{s,y}^2 + F_{s,z}^2}$$

$$\phi_{F,s} = \arccos\left(\frac{F_{s,z}}{\rho}\right)$$

$$\theta_{F,s} = \arctan\left(\frac{F_{s,y}}{F_{s,x}}\right) + \pi u_0(F_{s,x})$$

Giuseppe Cavallo

where u_0 stands for the Heaviside unit step function

$$u_0(x) = \begin{cases} 1 & \text{if } x \leq 0 \\ 0 & \text{if } x > 0 \end{cases} \quad (5.1)$$

Angle features $\phi_{T,s}$ and $\theta_{T,s}$ can be computed similarly from the mean torque vector to characterize the mean torque “direction”.

Angular deviation to mean effort

Beside features characterizing mean direction of efforts, the angular deviation of every effort sample within the analysis frame from the mean effort is computed. It is assumed that the distribution of these angular deviations depicts some specific pattern (sudden variations, lack of smoothness, etc) in the stroke patient movements. Given a recording, for the s -th sensor, the angular deviation $\delta_{F,s}[k]$ between the k -th force sample $(F_{s,x}[k], F_{s,y}[k], F_{s,z}[k])$, within the analysis frame $k = k_0, \dots, k_0 + N - 1$, and the mean force $(\bar{F}_{s,x}, \bar{F}_{s,y}, \bar{F}_{s,z})$ is computed as the inverse cosine of the normalized scalar product, i.e. the dot product of the corresponding unit-norm vectors,

$$\begin{aligned} \vec{a} &= (\bar{F}_{s,x}, \bar{F}_{s,y}, \bar{F}_{s,z}) \\ \vec{b} &= (F_{s,x}[k], F_{s,y}[k], F_{s,z}[k]) \\ \delta_{F,s}[k] &= \arccos \left(\frac{\vec{a} \cdot \vec{b}}{\|\vec{a}\| \|\vec{b}\|} \right) = \\ &= \arccos \left(\frac{\bar{F}_{s,x}F_{s,x}[k] + \bar{F}_{s,y}F_{s,y}[k] + \bar{F}_{s,z}F_{s,z}[k]}{\sqrt{\bar{F}_{s,x}^2 + \bar{F}_{s,y}^2 + \bar{F}_{s,z}^2} \sqrt{F_{s,x}[k]^2 + F_{s,y}[k]^2 + F_{s,z}[k]^2}} \right) \end{aligned}$$

Several features are computed in order to characterize the distribution of the angular deviations $\delta_{F,s}[k]$, $k = k_0, \dots, k_0 + N - 1$. The angular deviations can take values between 0 to π . First, the maximum value $Max(\delta_{F,s})$ is computed in order to characterize the support of the distribution. Next, the mean value $Mean(\delta_{F,s})$ and the standard deviation $Std(\delta_{F,s})$ are estimated in order to characterize the central tendency and the dispersion of the distribution, respectively. Then, the skewness $Skew(\delta_{F,s})$ and the kurtosis $Kurt(\delta_{F,s})$ are estimated in order to characterize the asymmetry and the peakedness of the distribution. Finally, the probability density function of the angular deviations is estimated using kernel-based method $KS(\delta_{F,s})$.

Giuseppe Cavallo

Besides characterizing the statistical distribution of the angular deviations of the sequence of force samples to the mean force within the time region of interest, the feature extraction aims also at modelling the time correlation of the sequence of angular deviations. Such information can be provided in a compact form as the coefficients of an auto-regressive (AR) model fitting to the sequence of angular deviations.

First order angular deviation

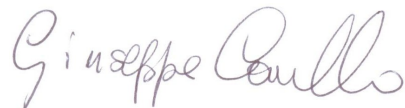
Additional information on stroke patient's ability in controlling generated forces / torques is expected to be found in the angular deviations between successive effort samples within the analysis frame. Given a recording, for the s -th sensor, the angular deviation $\phi_{F,s}$ between the k -th force sample ($F_{s,x}[k]$, $F_{s,y}[k]$, $F_{s,z}[k]$) and the $(k-1)$ -th force sample ($F_{s,x}[k-1]$, $F_{s,y}[k-1]$, $F_{s,z}[k-1]$), within the analysis frame $k = k_0 + 1, \dots, k_0 + N - 1$, is computed as the inverse cosine of the normalized scalar product, i.e. the dot product of the corresponding unit-norm vectors,

$$\begin{aligned} \vec{a} &= (F_{s,x}[k], F_{s,y}[k], F_{s,z}[k]) \\ \vec{b} &= (F_{s,x}[k-1], F_{s,y}[k-1], F_{s,z}[k-1]) \\ \varphi_{F,s}[k] &= \arccos \left(\frac{\vec{a} \cdot \vec{b}}{\|\vec{a}\| \|\vec{b}\|} \right) = \\ &= \arccos \left(\frac{F_{s,x}[k]F_{s,x}[k-1] + F_{s,y}[k]F_{s,y}[k-1] + F_{s,z}[k]F_{s,z}[k-1]}{\sqrt{F_{s,x}[k]^2 + F_{s,y}[k]^2 + F_{s,z}[k]^2} \sqrt{F_{s,x}[k-1]^2 + F_{s,y}[k-1]^2 + F_{s,z}[k-1]^2}} \right) \end{aligned}$$

Also in this case several statistical features were calculated (the same as in section 5.3.1). Besides characterizing the statistical distribution of the first-order angular deviations of the sequence of force samples within the time region of interest, the feature extraction aims also at modelling time correlation. Such information can be provided in a compact form as the order and the coefficients of an auto-regressive (AR) model fitting to the sequence of angular deviations.

Cumulative sum of effort series

The integrals of the effort signals are expected to convey some information on the velocity of the virtual movements (since the patient's movements are constraint by the ADD), thereof on the stroke patient ability to perform some movement velocity patterns. More especially, the norm of the integral of the



force/torque sample sequence is used. Given a recording, for the s -th sensor, the norm $\|\vec{\gamma}_{F,s}[k]\|$, $\vec{\gamma}_{F,s}[k]$ of the integral vector $\vec{\gamma}_{F,s}[k]$ of the force sample vector time instant, within the analysis frame $k = k_0, \dots, k_0 + N - 1$, is sequence at the k -th computed as the norm of the cumulative sum of the force sample vector from the k_0 -th time instant up to the k -th time instant,

$$\gamma_{F,s,x}[k] = \sum_{l=k_0}^k F_{s,x}[l]$$

$$\gamma_{F,s,y}[k] = \sum_{l=k_0}^k F_{s,y}[l]$$

$$\gamma_{F,s,z}[k] = \sum_{l=k_0}^k F_{s,z}[l]$$

$$\vec{\gamma}_{F,s}[k] = (\gamma_{F,s,x}[k], \gamma_{F,s,y}[k], \gamma_{F,s,z}[k])$$

$$\|\vec{\gamma}_{F,s}[k]\| = \sqrt{\gamma_{F,s,x}[k]^2 + \gamma_{F,s,y}[k]^2 + \gamma_{F,s,z}[k]^2}$$

Finally also for γ , the statistical features described above were calculated.

Note that it couldn't be considered like a real movement since the objects are fixed. A constant force implies a linear increase in speed under the imagined situation of free moving objects. In the situation of fixed objects, the usefulness of this parameter can be less pertinent, but it will serve as a kind of low-pass filtering on the data.

5.3.2 Onset detection

In order to be consistent with the first hypothesis of the ALLADIN paradigm for the assessment of the post-stroke recovery, the features are to be extracted within a time window beginning at the estimated onset of movement time for a given sensor. In agreement with the physiotherapists, the width of that window is finally set to 750 *ms* by the mean of a visual inspection of the force/torque measurements.

During muscle contractions a background vibration is present of which spectral components can reach 40 *Hz* in frequency. Spectral components resulting from voluntary movements have generally lower frequencies. Therefore, signals

Giuseppe Cavallo

are low-pass filtered at 40 *Hz* during the pre-processing step (10-order Butterworth filter). The part of signal within the analysis window is also normalized: subtraction of the first sample value and division by the last sample value.

Starting from the in-depth review of the state-of-the-art techniques and after an internal debate between engineers and clinical experts, candidate methodologies for automatic onset time estimation were identified by:

1. the point where the force-torque signal reaches 2% of its peak value;
2. using a 2nd order derivative of the force-torque signal (with low-pass filtering at 3 *Hz* or at 5 *Hz*);
3. using the Spectral Flatness Measure (SFM) of the force-torque signal, based on a maximal information redundancy criterion;
4. using a Probability Density Function (PDF) estimate of the force-torque signal through a kernel smoothing based method (ks-density).

A brief description of these techniques follows.

The 2% rule.

Former neuro-rehabilitation research inspired the proposed technique [136]. The input to the threshold-based algorithm consists of the three components of the force F_x , F_y and F_z (or torque) signals.

It computes the 2% of the peak value on the signal and finds the minimum time corresponding to that value for each component. This value is taken as onset time.

The second derivative method.

A previous study on the gait analysis inspired the present technique [137]. Three versions of the present algorithm (b, c, d) have been developed. The description of the single steps follows:

- a. it finds the threshold point on the 1st derivative of the input signal at the 15% of its maximum.
- b. it searches the nearest maximum peak of the second derivative of the 3 *Hz* filtered signal (2nd derivative-filtered 3 *Hz*).



- c. it searches the nearest maximum peak of the second derivative of the 5 Hz filtered signal (2nd derivative-filtered 5 Hz).
- d. it searches backward the zero crossing in the first derivative line (2nd derivative-zero crossing). This is similar to the 2% rule, except that it scans backward from a higher speed, so initial small velocity peaks are neglected.

The SFM method

The Spectral Flatness Measure (SFM) is a well-known method for quantifying the amount of randomness (or “stochasticity”) that is present in a signal. This measure has been widely used in signal compression, audio characterization and retrieval.

SFM is defined as the ratio of the geometric mean to the arithmetic mean of the power spectral components in every spectral band. Sometimes called also “tonality coefficient”, it is used to quantify how much tone-like a sound is, as opposed to being noise-like.

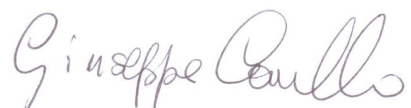
It can be shown that $0 < SFM < 1$. $SFM = 0$ corresponds to structured or non-random process, while $SFM = 1$ corresponds to a random signal in the sense that no extra information can be obtained by looking at longer blocks of signal samples, i.e. having no additional structure when considering these measurements as a “process”.

The SFM method is thoroughly described in [109].

In this application SFM is used to detect when the signal stops to be a noise-like signal (rest position). In particular when the Spectral Flatness becomes smaller than a predefined threshold, conventionally this is considered as the movement initiation point. The use of the measure in this application is motivated by the fact that once the subject intends to perform the movement, the recorded signals become less random.

The kernel smoothing based method (ks-density).

The ks-density function computes a PDF estimate of the input vector. Typically stationary values (e.g. flat regions) of force-torque signal correspond to maxima of the PDF while values where the slope of the signal is high generally correspond to minima of the PDF. The algorithm locates the minimum of the local minima (Minimum Density Point, MDP) in the ks-density function [138]. A first version of the PDF estimation algorithm outputs the MDP as the onset time. In the second version, a line passing through the MDP (green line in



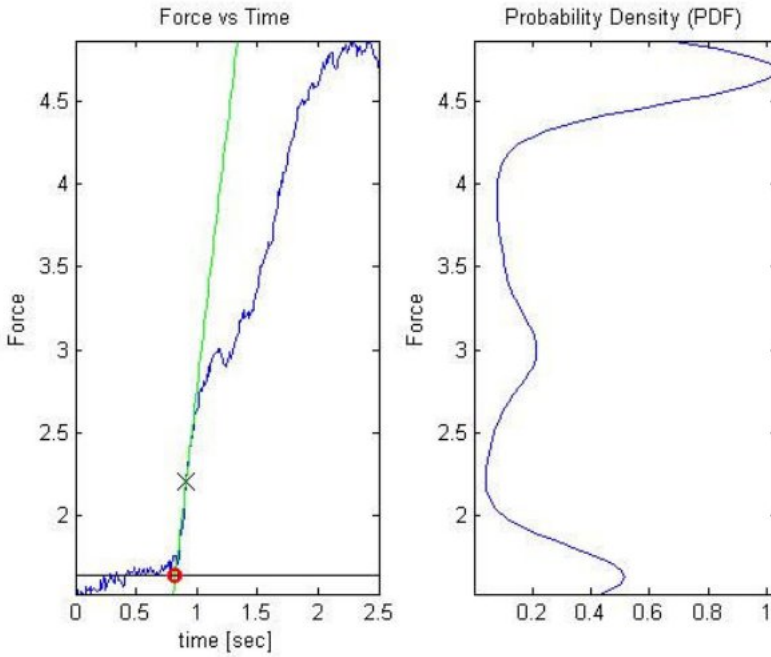


Figure 5.3: Application of the ks-density based technique on a sample force measurement

Fig.5.3) is drawn with a slope equal to the mean value of the first derivatives of an interval around the MDP. The ks-density also allows calculating the mean value of the signal before the task starts that generally corresponds to the first maximum in the PDF. The onset point is then determined when the tangent crosses this threshold value. The application of the ks-density based technique is illustrated in Fig.5.3.

5.4 Comparative evaluation and results

In order to evaluate what is the best onset detection technique, a patient/normal control balanced force/torque measurement data subset was manually selected. The selection was performed by a visual inspection of the signals. It is impor-

Giuseppe Cavallo

Onset technique	Mean value	Standard deviation	Variance	Median	POC
2% rule	0.5080	0.8524	0.7266	0.3887	0.57
Spectral flatness	0.0968	0.7870	0.6194	0.0990	0.69
Ks-density (interpolation)	-0.0252	0.7959	0.6335	-0.1766	0.71
2nd derivative (filtered 3Hz)	0.2136	0.6223	0.3873	-0.0188	0.89
2nd derivative (filtered 5Hz)	0.2044	0.6241	0.3894	-0.0276	0.89

Table 5.3: Results of the comparative study of different onset of movement detection methods. Mean value, standard deviation, variance and median are related to the error distribution. The mean absolute value is the mean of the error absolute value distribution.

tant to highlight that no information about the patients' profile group was used. so to guarante the subselection to be representative of the global database.

Then the subselection was distributed to the clinical experts in order to understand more in details how they decide which time point in the signal corresponded to the onset of the signal related to the execution of the ADL task. It has been discovered that they used a more sophisticated analysis, when compared to the results obtained by the calculated onset. They gave a physiological interpretation to the signals, which became reflected in the way the onset time was tagged.

The dataset used to assess the performance of the onset of movement time detection algorithm, contained data from 96 patients (48 patients and 48 normal controls), all selected from the proof of concept database.

Table 5.3 presents the results of the comparative analysis among the per-



performances of the different candidate techniques with respect to the reference performance of three clinical experts. First, the Mean Reference Vector (MRV) has been derived by the experts inputs by computing the mean value of the three onset times estimated by the three experts for each of the measurements. Then, Mean value, Standard Deviation, Variance and Median of the error vector related to each of the candidate techniques have been calculated (columns 2-5). Finally, also a non-parametric statistical feature, defined as the Probability Of Correctness (POC), has been computed. POC is calculated as the ratio N_c/N , where N is the total number of samples and N_c is the number of samples which fall between the 5th-percentile and the 95th-percentile of the MRV.

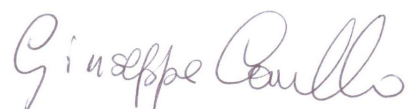
The analysis on the dataset has enlightened the following results:

1. Techniques based on application of thresholds to the 2nd-derivative of the force/torque signals demonstrate the best performance among the selected candidate techniques;
2. all the four proposed onset detection techniques work properly for detecting the onset in terms of Signal to Noise Ratio;
3. the proposed techniques can be used to remove those parts of the signal which are useless;
4. the first phase of the data mining stage should be dedicated to the identification and recognition of typical pattern, which then could allow a narrower time windowing.

5.4.1 The ALLADIN pre-processing tool

The algorithms described above have been implemented in Matlab environment as libraries to be included in a more general software. Here a brief description of its structure follows.

The Alladin Pre-processing Tool (APT) is a software tool that automatically derives specific parameters from the ADD recordings; store the output data into a structure using a format for subsequent data mining analysis that has to lead to the extraction of clinical markers and milestones, relevant for functional assessment of patients. The APT also includes a Visualization Module which allows visual inspection of data during the pre-processing operations.



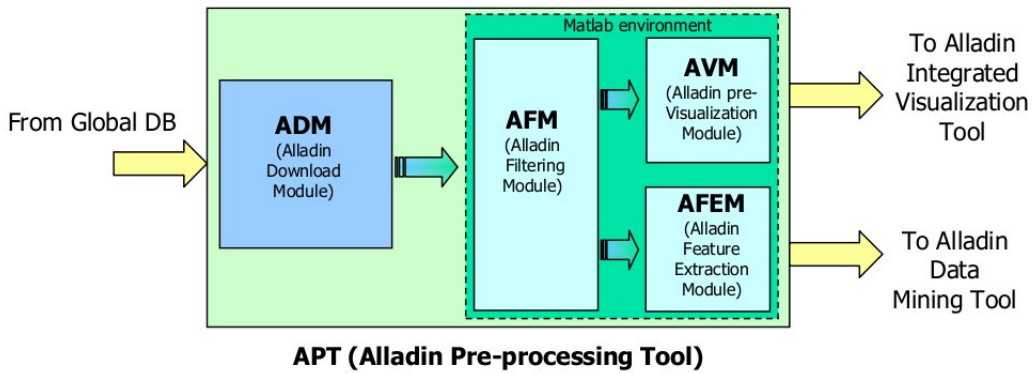


Figure 5.4: Overall architecture of the APT - Alladin Pre-processing Tool

5.4.2 The ALLADIN filtering module (AFM)

A two-channel parallel low-pass filtering, one featuring a cut-off frequency at 40 Hz and another with a cut-off frequency at 2 Hz was proposed and implemented in order to provide two separate data sets for subsequent processing. The two cut-off frequencies were selected taking into account that, on one hand, human muscles can generate mechanical signals up to a maximum frequency of 40 Hz (muscle sound) [139], while, on the other hand, human voluntary movement typically generates signals within the frequency range $0 - 2\text{ Hz}$ [140]. The 40 Hz -channel is the main channel used for feature extraction, while the 2 Hz -channel is used for visualization and onset time estimation operations.

5.4.3 The ALLADIN previsualization module (AVM)

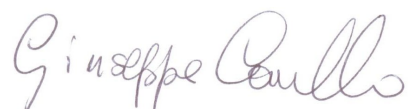
The ALLADIN Visualization Module (AVM) was developed in order to visualize the ALLADIN measurements. Through the controls positioned on the main window, the patient ID, session, task and measurement number can be selected. Data filtering, calculations (minimum, maximum, mean) and coordinate transformations can be applied to the measurements, and plotted for inspection. A slightly different version of AVM was implemented with the aim of simplifying the clinical experts' task. The module allows manual selection of the onset time directly on the plot, by simply clicking on the window by using the PC mouse.

Giuseppe Cavallo

5.4.4 The ALLADIN feature extraction module (AFEM)

The Alladin Feature Extraction Module (AFEM) receives the filtered data from the 40 Hz-filtered channel of the AFM and generates the output data containing statistical and temporal features calculated for all the ADD measurements of the input data set. The AFEM computes the complete list of parameters based on the assumptions and the definitions previously described. The APT generates, through the AFEM module, an output data structure variable (named 'F.Features'). The extracted parameters for every recording were stored in the above hierarchical structure of strings, arrays and cell arrays containing the identification information as well. Every stored parameter presented a description and a value. As mentioned in the previous paragraphs, a small subset of six features has been extracted from the original set of parameters, which contains a huge amount of data. The criterion for these features selection was their clinical relevance. A description of the extracted features follows:

1. Standard deviation value of the integral of the sample vector within the time region of interest, in the middle finger sensor during the second attempt of the drinking task.
2. Maximum value of the angular deviation between the torque sample vector and the mean torque vector within the time region of interest, in the thumb finger sensor during the fourth attempt of the lifting bottle task.
3. Mean value of the angular deviation between the torque sample vector and the mean torque vector within the time region of interest, in the seat sensor during the third attempt of the drinking task.
4. Standard deviation value of the integral of the sample vector within the time region of interest, in the thumb finger sensor during the fourth attempt of the lifting bottle task.
5. Normalized sum of the residual, in the thumb finger sensor during the fourth attempt of the drinking task.
6. Mean value of the angular deviation between the force sample vector and the previous force vector within the time region of interest, in the index finger sensor during the fourth attempt of the lifting bag task.



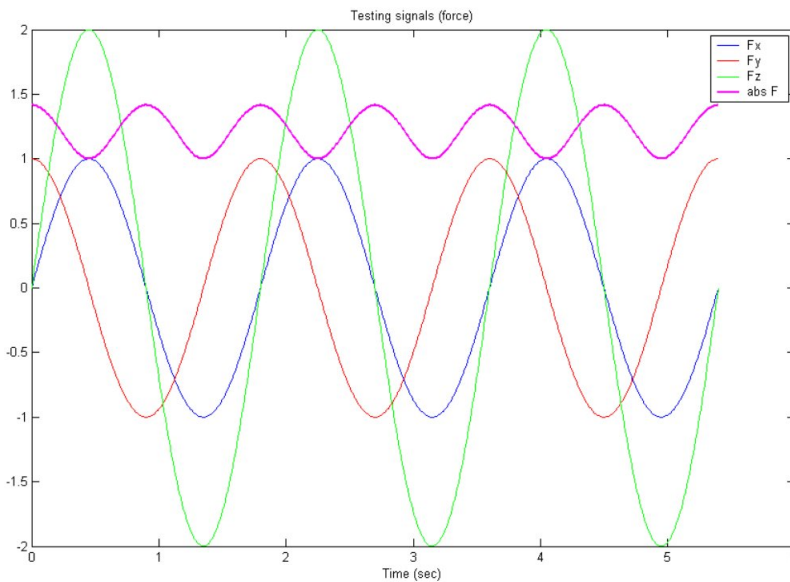


Figure 5.5: Testing signals for the force components

5.4.5 APT testing

Test signals were created by Matlab scripts: for each Cartesian reference axis (x , y , z), force and torque trigonometric signals having a length of of 400 ms were generated. The choice of such signals (sine and cosine with different amplitudes) and the relative time interval (6π) is adequate for reproducing a signal with three peaks, ideally corresponding to the three repetitions of the typical recording during a measurement session (Fig.5.5). Each test signal was passed as input vector to the AFEM and the output vector was compared with the explicit calculation of the statistical parameters. As expected, a null vector was been obtained as the difference between the previous two vectors. The test was performed for both force and torque signals. The results obtained from the tests performed on the AFEM module, after its validation, suggests that the AFEM module properly calculates all the parameters defined so far.

Giuseppe Cavallo

5.5 Conclusion

This chapter describes the design methodology and the application of a clinical data pre-processing software tool. As an example, an application to a mechatronic platform for whole-body isometric force-torque measurements for functional assessment in neuro-rehabilitation was presented. Thanks to the close collaboration between medical doctors (physiotherapists, neurologists, etc.) and biomedical engineers, after several clinical tests, a multidisciplinary approach was proposed to simplify the problem of handling the great amount of acquired raw data. In the proposed approach the relevant part of the raw signal (i.e., the part in which the force-torque exerted by the patient is clearly visible) was selected through the use of a series of movement onset detection algorithms. Then a first set of parameters were extracted as possible feature candidates in a preprocessing stage. These pre-elaborated data input to data mining, will strongly decrease the computational workload. The thorough analysis performed during this work will be used to further investigate if specific body segments are involved during particular tasks and/or if the addition of one or more sensors to the platform could provide further useful dynamic information. All this information will lead to a possible re-design of the platform, with the aim to improve the present version of the device for functional assessment and for basic research in the neuroscience domain as well.

Giuseppe Cavallo

Conclusions

This dissertation summarizes the author's research activities during his PhD. The main research topic deals with the use of mechatronic technologies for the analysis of behaviour both in animal models and in human. The work presented is organized with a preliminary introduction explaining motivations and main focuses of the research; then a series of cases-study follow, showing different possible applications in which medical activities (base research, diagnosis, pharmacological or rehabilitation treatments, ecc) gain benefit by the integration of mechatronic tools.

In the Introduction the relationship between Mechatronics and Behavioural Analysis (in its wider significance) was explored: behavior is anything a person or animal does that can be measured [9] and Mechatronics can provide methods and techniques to perform this in an unbtrosive and ecological way. One typical medical research field addressed by behavioural analysis is Genetics, more particularly Phenomics, whose aim is to study subtle genetic modifications under a functional viewpoint by analyzing the subsequent behaviour alterations. To this regard particularly useful are animal models of human pathologies since they allow in vivo tests which are much more reliable than simulation or mathematical models. Animal models are widely used also for Neuroscience research: typical features of human neurological or neurodevelopmental disorders are simplified in models so to assess drugs or neurorehabilitation treatments.

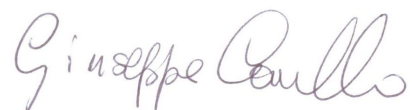
The second chapter presents a mechatronic force detecting platform for tremor analysis in small animal models (i.e. mice). The innovative aspects of the platform are the capability of detecting *horizontal* components of forces exerted by a *single mouse paw*. The device integrates different sensors for a wide multimodal analysis: the main one is a Ground Reaction Force sensor detecting directly mouse paws tremor; then a MEMs inertial sensor (i.e. accelerometer) is used for in-situ calibration purposes. Indeed, as also explained in Chapter 3, most of times behavioural analysis experiments are performed in



non-engineering labs by medical researchers, thus implying the need for simple, fast and low-cost calibration procedures not requiring high quality costly instrumentations. Finally a CCD camera has been also added to the device heading at mouse's paw plant, so to understand when the mouse is effectively stepping over the platform and to refer the tremor detected to mouse orientation. The platform has been tested on reeler mice, an animal model of a human neurodevelopmental disorder, the Autism. Reelers are affected by ataxia and an evident paw tremor that have never been quantified before. Preliminary experimental tests performed on reelers showed the presence of that tremor and allowed its dynamic characterization.

In the third chapter another mechatronic platform for movement analysis is presented. This platform allows the study of the correlation between movement planning and actual movements in catching tasks. It provides kinematic and dynamic measurements from the wrist and EEG and EMG signals of the tester. The task to be performed consists in the catching and grasping of a moving handle, sliding on a low friction rail. The handle is driven by a precharged spring. 10 subjects were tested according a protocol defined in collaboration with neurologists. Also in this case features have been defined and extracted from raw signals to simplify the assessment of results and to obtain indices handy to adopt in clinical practice. In particular preliminary analysis on EEG confirmed what reported in literature about the cortical activation areas during complex tasks while the analysis on kinematic data showed an improvement of motor performances after a first set of tasks that was interpreted in terms of motor learning.

The fourth chapter expands the experience of what has been done with reeler mice, introducing a new research field, the *Neurodevelopmental Engineering*. This discipline is strongly multi-disciplinar, integrating different competencies such as Engineering, Neuroscience, Psychology, etc... It aims at quantitative analysis and modeling of human behaviour during neural development to understand or discover the causes of behavioural disorders. So while for animal models researchers are forced to define and analyze simplified behavioural traits (i.e. physiological measurements) scaling down more complex human behaviours, in this case higher level human qualities such as expression of emotions or social communication can be directly studied through the use of Mechatronics which allows the adoption of unobtrusive and ecological devices aiming at not altering the natural behaviour of the tester. To this regard, finally a new simple low-cost procedure for in-field calibration of orientation magneto/inertial sensors is presented, explaining the underlying mathematical theory and showing calibration results demonstrating the effectiveness of the



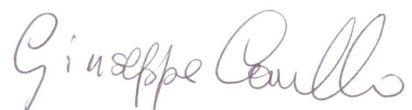
proposed method.

The fifth chapter focuses on an application of behavioural analysis for Neuro-rehabilitation. The mechatronic platform used in this work is briefly presented: it's a force/torque detecting system for isometric measurements in Activities of Daily Living tasks whose target are neurological patients in particular post-stroke. The importance of isometric measurements in clinical practice and for research purposes was discussed in the chapter: the initiation of a task has the same functional properties as performing the task [106, 107, 110, 111] and, since in first days after the stroke, movements are very limited, this approach could help in assessing the patient's neurological conditions and also the progress of rehabilitation recovery. The final goal is to identify predictive clinical markers of patient clinical evolution, thus quantifying (making subjective) it. The platform generates a huge amount of raw data, so that a reduction of information to manage is highly desirable. In the chapter a discussion on feature definition and extraction and techniques for onset detection are reported. In particular concerning the onset detection, different methods are tested and compared to onset values selected by clinical experts. Finally the best method is choice following results obtained from tests.

All these cases-study have a common background: they focus on physiological parameters related to kinematics of human or animal behaviour. Infact, in the second chapter, tremor and ataxia during mouse gait are analyzed; the third chapter presents an application towards the analysis of the kinematics in the manipulation of an object performed by autistic children; the fourth chapter constitutes an exception: isometric measurement means no movement, but the underlying working hypothesis is that kinematic features of a voluntary task can be extracted from the initial instants, when no actual movement was still performed; finally the fifth chapter deals with the analysis of kinematics of a common grasping task.

This work attests how large and productive the integration of Mechatronics with Behavioural Analysis can be. In modern and globalized science the need for comparison of results among different laboratories around the world implies measurement processes to be highly reliable and repeatable (i.e. objective). These achievements can be completely fulfilled by using modern technologic devices, but in applications (such as Behavioural Analysis) where tools obstruction (i.e. weight, dimensions) and ecology of experimental environment become a major issue, classic technologies may fail. In this scenario Mechatronics takes place providing an integrated approach aiming at the improvement of the existing solutions or even enabling new strategies for their achievement.

So basing on the research experiences reported in this dissertation, the role



of Mechatronics in medical research and practice can be synthesized as:

improvement of the existing analysis of biological data (i.e. behaviour) in particular **i. *expanding*** the multimodality of the measurement to discover possible correlations among different physiological parameters or **ii. *enhancing*** the quality of the single measurement (i.e. reliability, spatial or temporal resolution and precision, simple and high quality calibrations, etc)

enabling innovative solutions in monitoring and studying behavioural features that have never been studied opening new ways to the diagnosis and the treatment of still incurable human pathologies.

Giuseppe Cavallo

List of Publications

Published

D. Campolo, G.Cavallo, F.Keller, D.Accoto, P.Dario, E.Guglielmelli, “*A mechatronic system for in-plane Ground-Reaction-Force measurement for tremor analysis in animal models*”, IROS 2005, IEEE/RSJ International Conference on Intelligent Robots and Systems, pp. 2505-2510, Alberta, Canada, 2005

D. Campolo, G. Cavallo, F. Keller, D. Accoto, P. Dario, E. Guglielmelli, “*Design and development of a miniaturized 2-axis force sensor for tremor analysis during locomotion in small-sized animal models*”, EMBC 2005, The 27th Annual International Conference of the IEEE Engineering in Medicine and Biology Society, pp. 5054-5057, Shangai, China, 2005.

D. Campolo, G. Cavallo, E. Guglielmelli, F. Keller, “*A mechatronic system for tremor analysis in reeler mice via in-plane Ground-Reaction-Force measurement*”, Neuroscience 2005, the Societys 35th annual meeting, Washington, USA, 2005

D. Campolo, M.Fabris, G. Cavallo, D.Accoto, F.Keller, E.Guglielmelli, “*A novel precedure for In-field Calibration of Sourceless Inertial/Magnetic Orientation Tracking Wearable Devices*”, The 1st IEEE/RAS-EMBS International Conference on Biomedical Robotics and Biomechatronics, pp. 471-476, 2006



G. Cavallo, D. Campolo, E. Guglielmelli, S. Vollaro, F. Keller, "*Mechatronics and Phenomics: a case-study on tremor detection during locomotion in small-sized animals*", BioRob 2006, The first IEEE / RAS-EMBS International Conference on Biomedical Robotics and Biomechatronics, pp. 595-600, Pisa, Italy, 2006

D. Campolo, S. Sapir, G. Cavallo, F. Taffoni, E. Guglielmelli, F. Keller, "*Design and Development of a Mechatronic rattle for the Sonification of Infants Movements for Early Detection of Developmental Disorders*", the 2007 IEEE International Conference on Robotics and Automation (ICRA), Rome, Italy.

S. Mazzoleni, G. Cavallo, M. Munih, J. Cinkelj, M. Jurak, J. Van Vaerenbergh, D. Campolo, E. Guglielmelli, "*Towards application of a mechatronic platform for whole-body isometric force-torque measurements to functional assessment in neuro-rehabilitation*", 2007 IEEE International Conference on Robotics and Automation (ICRA), pp. 1535-1540, Rome, Italy, 2007

In press

G. Cavallo, D. Campolo, F. Keller, E. Guglielmelli, "*A modular platform for in-plane Ground Reaction Forces detection in mouse model: design, development and verification*", in press Advanced Robotics, 2008

G. Cavallo, D. Campolo, G. Fogliani and E. Guglielmelli, "*A novel method for in-situ calibration of a 2-dof force platform for tremor detection in small-sized animal models*" accepted for 2008 IEEE International Conference on Robotics and Automation (ICRA), California, 19-23 May 2008

Submitted

L. Zollo, G. Cavallo, E. Cattin, F. Zappasodi, M. Tombini, M.C. Carrozza, P.M. Rossini, E. Guglielmelli, "*Design and development of a platform for studying interception and catching tasks*", submitted to IEEE Transactions on Neural Systems and Rehabilitation Engineering, 2008.

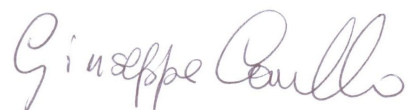


P.Soda, G.Cavallo, S.Mazzoleni, E.Guglielmelli, G.Iannello, “*A supervised pattern recognition approach for human movement onset detection*” submitted to The 21th IEEE International Symposium on Computer-Based Medical Systems (CBMS)

In preparation

S. Mazzoleni, A. Toth, M. Munih, J. Van Vaerenbergh,, G. Cavallo, P. Dario and E. Guglielmelli “*Dynamometric platform for whole-body isometric measurements as functional assessment tool in neurorehabilitation*” in submission to IEEE Transactions on Neural and Rehabilitation Systems Engineering (TNSRE)

Stefano Mazzoleni, Giuseppe Cavallo, Marko Munih, Justin Cinkelj, Andras Toth, Mihaly Jurak, Jo Van Vaerenbergh, Paolo Dario and Eugenio Guglielmelli, “*Design Methodology and Application of an Electronic Health Record Software and Clinical Data Analysis Tools in a Diagnostic Platform to Functional Assessment in Neuro-rehabilitation*”

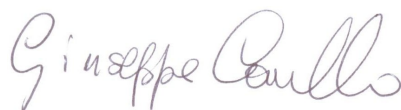


Tesi di dottorato in Ingegneria Biomedica, di Giuseppe Cavallo,
discussa presso l'Università Campus Bio-Medico di Roma in data 08/02/2008.
La disseminazione e la riproduzione di questo documento sono consentite per scopi di didattica e ricerca,
a condizione che ne venga citata la fonte.

Giuseppe Cavallo

Bibliography

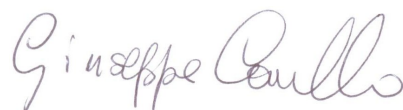
- [1] IRDAC, Opinion on R&D needs in the field of Mechatronics, Industry R&D Advisory Committee of the Comm. of the EC, Brussels, Belgium, 1986
- [2] van Amerong, Mechatronics in biomedical applications and biomechatronics, Proceedings of International Biomechatronics Workshop, Enschede, The Netherlands, pp. 105-109, April 1999
- [3] van Brussel, H. The Mechatronics approach to motion control. In proc. of the Int. Conf. on Motion control -The Mechatronics approach, Oct. 1989, Atwerp Belgium
- [4] Shetty, D., Kolk R. A., Mechatronics system design. PWS Publishing Company, 1997, ISBN 0-534-95285-2.
- [5] Hewitt, R. Mechatronics - the contributions of advanced control. In proc. of 2nd Conference on Mechatronics and Robotics. Duisburg/Moers, Germany, September 27-29, 1993.
- [6] Jan Wikander and Martin Torngren, Mechatronics as an engineering science, in Proc. of Mechatronics 98 Int. Conference, published by Elsevier Science Ltd. ISBN 0-08-043339-1
- [7] S. E. Lyshevski, Mechatronic curriculum- retrospect and prospect, Mechatronics 12 (2002) 195-205
- [8] H. Witte, S. Lutherdt and C. Schilling, Biomechatronics How much biology does the engineer need?, Proceedings of the 2004 IEEE International Conference on Control Applications Taipei, Taiwan, September 2-4, 2004
- [9] Association for Behavior Analysis International, 1219 South Park Street Kalamazoo MI 49001 Phone: (269) 492-9310 Fax: (269) 492-9316 E-mail: mail@abainternational.org, WebSite: <http://www.abainternational.org>



- [10] Cambridge Center for Behavioural Study, 336 Baker Avenue Concord, Massachusetts U.S.A. 01742-2107, Phone: (978)369-CCBS (2227), Fax: (978) 369-8584, WebSite: <http://www.behavior.org>
- [11] Paul Martin, Patrick Bateson, *Measuring Behaviour: An Introductory Guide*. Psychometrics, Cambridge University Press, 1993
- [12] B. R. Bochner, New technologies to assess genotype–phenotype relationships, *Nature Reviews Genetics*, Vol.4, pp.309-314, April 2003
- [13] J. N. Crawley, Behavioral Phenotyping of Rodents, Vol.53, No.2, *Comparative Medicine* April 2003
- [14] F. J. van der Staay, T. Steckler, Behavioural phenotyping of mouse mutants, *Behavioural Brain Research*, Vol.125 pp. 3–12, 2002
- [15] M. Bucan and T. Abel, The mouse: Genetics meets behaviour, *Nature Review Genetics*, Vol.3 pp.114-123, Feb 2002
- [16] J. Harris, Behavioral phenotypes of neurodevelopmental disorders: portals into the developing brain, In: K. L. Davis, *Neuropsychopharmacology: The Fifth Generation of Progress*, Lippincott Williams & Wilkins, 2002
- [17] J. Harris, Introduction to behavioral phenotypes. In: Harris J, ed. *Assessment, diagnosis and treatment of the developmental disorders*, pp.245–249 New York, Oxford University Press, 1998
- [18] Flint J, Yule W. Behavioural phenotypes. In: M. Rutter, E. Taylor, L. Hersov, eds. *Child and adolescent psychiatry*, third ed. Oxford Blackwell Scientific, pp.666–687, 1994.
- [19] S.D. Brown, J. Peters, Combining mutagenesis and genomics in the mouse - closing the phenotype gap. *Trends Genet.* Vol.12, pp.433–435, 1996
- [20] Crawley, J. N. *What's wrong with my mouse? Behavioral phenotyping of transgenic and knockout mice*. John Wiley & Sons, Inc., New York, 2000.
- [21] Campbell, I. L. and L. H. Gold. Transgenic modeling of neuropsychiatric disorders. *Mol. Psychiatr.* 1:105-120, 1996.
- [22] J. Flint. R. Corley, Do animal models have a place in the genetic analysis of quantitative human behavioural traits?, *J Mol Med*, Vol.74, pp.515-521, 1996

Giuseppe Cavallo

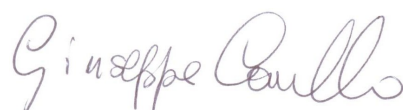
- [23] Crawley, J.N. and Paylor, R., A proposed testbattery and constellation of specific behavioral paradigms to investigatethe behavioral phenotypes of transgenic and knockout mice. *Horm. Behav.*31, 197–211, 1997
- [24] R.Gerlai, Phenomics: fiction or the future?,*TRENDS in Neurosciences*, Vol.25, No.10 October, 2002
- [25] D. Graham, A behavioural analysis of the temporalorganisation of walking movements in the 1st instar and adult stickinsect (*Carausius morosus*), *Journal of Comparative Physiology A: Neuroethology, Sensory, Neural, and Behavioral Physiology*, Vol.81,N.1, pp.23-52,1972
- [26] R. Morris, Developments of a water-maze procedurefor studying spatial learning in the rat, *Journal of NeuroscienceMethods*, 11, 47-60, 1984
- [27] L. M. McQuoid & B. G. Galef, Social stimuliinfluencing feeding behaviour of Burmese fowl: a video analysis, *Anim.Behav.*, 46,13-22, 1993
- [28] D. Campolo, C. Laschi, F. Keller, E. Guglielmelli,A mechatronic platform for early diagnosis of neurodevelopmental disorders,*Advanced Robotics*, Vol. 21, No. 10, pp. 1131- 1150, 2007
- [29] S. Park, I. Locher, A. Savvides, M. B. Srivastava, A. Chen, R. Muntz, S. Yuen, Design of a Wearable Sensor Badge forSmart Kindergarten, *Proceedings of the 6th International Symposiumon Wearable Computers (ISWC'02)*, 2002
- [30] J. Farrington, A. J. Moore, N. Tilbury,J. Church, P. D. Biemond, Wearable Sensor Badge and Sensor Jacketfor Context Awareness, *Third International Symposium on Wearable Computers(ISWC'99)* p. 107, 1999
- [31] LeDoux, J. E. Emotion circuits in the brain.*Annu. Rev. Neurosci.* 23, 155–184 (2000)
- [32] Waelti, P., Dickinson, A. & Schultz, W. Dopamineresponses comply with basic assumptions of formal learning theory.*Nature* 412, 43–48 (2001).
- [33] Impagnatiello F, Guidotti AR, Pesold C, Dwivedi Y, Caruncho H, Pisu MG et al. A decrease of Reelin expression as a putative vulnerability factor in schizophrenia. *Proc Natl Acad Sci USA* 1998; 95:15718-15723.



- [34] Fatemi SH, Earle JA, McMenomy T. Reduction in Reelin immunoreactivity in hippocampus of subjects with schizophrenia, bipolar disorder and major depression. *Mol Psychiatry* 2000; 5: 654-663.
- [35] Keller F, Persico AM, Zelante L, Gasparini P, D'Agruma N, Maiorano N et al. Reelin gene alleles and haplotypes are associated with autistic disorder. *Soc Neurosci* 2000; 26: 77 (31.11).
- [36] Persico AM, D'Agruma L, Maiorano M, Totaro A, Militerni R, Bravaccio C et al. Reelin gene alleles and haplotypes as a factor predisposing to autistic disorder. *Mol Psychiatry* 2001; 6: 150-159.
- [37] Bothwell M, Giniger E. Alzheimer's disease: neurodevelopment converges with neurodegeneration. *Cell* 2000; 102: 271-273
- [38] G.D'Arcangelo, T.Curran, Reeler: new tales on an old mutant mouse, *BioEssays* 20:235-244,1998.
- [39] Goffinet AM. An early developmental defect in the cerebral cortex of the Reeler mouse. *Anat Embryol* 1979; 157: 205-218.
- [40] DeSilva U, D'Arcangelo G, Braden VV, Chen J, Miao G, Curran T, Green ED (1997) The human reelin gene: Isolation, sequencing, and mapping on chromosome 7. *Genome Res* 7:157-164.
- [41] P. Dario, C. Laschi, A. Menciassi, E. Guglielmelli, M. C. Carrozza, S. Micera, Design and development of a neurobotic human-like guinea pig, *Engineering in Medicine and Biology, 2002. 24th Annual Conference and the Annual Fall Meeting of the Biomedical Engineering Society*, Vol. 3, pp. 2345-2346, Houston, Texas, October 23-26, 2002.
- [42] P. humansDario, M.C. Carrozza, E. Guglielmelli, C. Laschi, A. Menciassi, S. Micera, F. Vecchi, Robotics as a Future and Emerging Technology: Biomimetics, Cybernetics and Neuro-Robotics in European Projects, *IEEE Robotics and Automation Magazine*, Vol. 12, No. 2, pp. 29-45 2005
- [43] R. Gerlai, Phenomics: fiction or the future?, in *Trends in Neurosciences*, Vol. 25, No. 10, pp. 506-509, 2002
- [44] H. Steinberg, E. A. Sykes, A. McBride, P. Terry, K. Robinson and H. Tillotson, Computer Analysis, Using a Digitizer, of Ataxic Mouse Gait Due to Drugs, *Journal of Pharmacological Methods* Vol. 21, No. 2, pp. 103-113, 1989.

Giuseppe Cavallo

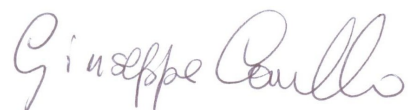
- [45] A. Biewener and R.J. Full, Force platform and kinematic analysis, in *Biomechanics: Structures and Systems, A Practical Approach.*, pp 45-73, IRL at Oxford University Press, New York, 1992.
- [46] K.A. Clarke, J. Still, Gait Analysis in the Mouse, *Physiology & Behavior*, Vol. 66, No. 5, pp. 723-729, 1999.
- [47] S.C. Fowler, Behavioral "Spectroscopy" with the Force-Plate Actometer, *Current Separations*, Vol. 20, No. 1, pp. 17-22, 2002.
- [48] D.E. Handley, J.F. Ross and G.J. Carr, A Force Plate System for Measuring Low-Magnitude Reaction Forces in Small Laboratory Animals, *Physiology & Behavior*, Vol. 64, No. 5, pp. 661-669, 1998.
- [49] G.D. Muir and I.U. Wishaw, Complete locomotor recovery following corticospinal tract lesions: measurement of ground reaction forces during overground locomotion in rats, *Behavioral Brain Research*, Vol. 103, No. 1, pp. 45-53, 1999.
- [50] Boose, A., Spieker, S., Jentgens, C., & Dichgans, J., Wrist tremor: investigation of agonist -antagonist interaction by means of long-term EMG recording and cross-spectral analysis. *Electroencephalography and Clinical Neurophysiology*, 101, 355-363, 1996.
- [51] Baker, D., Pryce, G., Croxford, J. L., Brown, P., Pertwee, R. G., Huffman, J. W., & Layward, L., Cannabinoids control spasticity and tremor in a multiple sclerosis model. *Nature*, 404, 84-87, 2000.
- [52] Gunther, H., Brunner, R., & Klussmann, F. W., Spectral analysis of tremorine and cold tremor electromyograms in animal species of different size. *Pflügers Archiv*, 399, 180-185, 1983.
- [53] Ackmann, J. J., Sances, A. Jr., Larson, S. J., & Baker, J. B., Quantitative evaluation of long-term parkinson tremor. *IEEE Transactions on Bio-Medical Engineering*, 24, 49-56, 1977.
- [54] Christakos, C., Lal, S., Mathams, R. F., & Rawstorne, I., Threedimensional measurement of finger tremor. *Journal of Physiology*, 270, 8-9, 1977.
- [55] Boyd, W., & Lakie, M., Aperiodic tremor of the human finger. *Journal of Physiology*, 380 (3 pp.), 1986.



- [56] Norman, K. E., Edwards, R., & Beuter, A., The measurement of tremor using a velocity transducer: comparison to simultaneous recordings using transducers of displacement, acceleration and muscle activity. *Journal of Neuroscience Methods*, 92, 41-54, 1999.
- [57] Sinclair, K. G., Honour, A. J., & Griffiths, R. A., A simple method of measuring tremor using a variable-capacitance transducer. *Age and Ageing*, 6, 168-174, 1977.
- [58] Frost, J. D. Jr., Triaxial vector accelerometry: a method for quantifying tremor and ataxia. *IEEE Transactions on Bio-Medical Engineering*, 25, 17-27, 1978.
- [59] Hallberg, H., Carlsson, L., & Elg, R. J., Objective quantification of tremor in conscious unrestrained rats, exemplified with 5-hydroxytryptamine-mediated tremor. *Journal of Pharmacological Methods*, 13, 261-266, 1985.
- [60] Clement, J. G., & Dyck, W. R., Device for quantitating tremor activity in mice: antitremor activity of atropine versus soman- and oxotremorine-induced tremors. *Journal of Pharmacological Methods*, 22, 25-36, 1989.
- [61] Gilbert, J. A., Maxwell, G. M., McElhaney, J. H., & Clippinger, F. W., A system measure the forces and movements at the knee and hip during level walking. *Journal of Orthopaedic Research*, 2, 281-288, 1984.
- [62] Falconer DS, Two new mutants "trembler" and "reeler" with neurological actions in the house mouse. *J Genet* 50:192-201, 1951.
- [63] G.D. Muir, I.Q. Whishaw, Ground reaction forces in locomoting hemiparkinsonian rats: a definitive test for impairments and compensations, *Experimental Brain Research*, Vol. 126, pp. 307-314, 1999.
- [64] L.L.Cai, A.J.Fong, Y. Liang J.Burdick, C.K.Otoshi and V.R.Edgerton, Effects of Assist-as-needed Robotic Training Paradigms on the Locomotor Recovery of Adult Spinal Mice, *The 1st IEEE / RAS-EMBS International Conference on Biomedical Robotics and Biomechanics.*, Pisa, 2006
- [65] M.S. Young, C.W. Young, Y.C. Li, A combined system for measuring animal motion activities, *Journal of Neuroscience Methods* Vol. 95, No. 1, pp. 55-63, 2000.
- [66] R.H. Bishop, *The Mechatronics Handbook*, CRC Press, 2002.

Giuseppe Cavallo

- [67] L.L. Howell, *Compliant Mechanisms*, John Wiley & Sons, Inc., 2001.
- [68] H. Wilms, J. Sievers, G. Deuschl, Animal Models of Tremor, *Movement Disorders Soc.*, Vol. 14, No. 4, pp. 557-571, 2001.
- [69] D. Campolo, G. Cavallo, F. Keller, D. Accoto, P. Dario, E. Guglielmelli, A mechatronic system for in-plane ground-reaction-force measurement for tremor analysis in animal models, *2005 IEEE/RSJ International Conference on Intelligent Robots and Systems, 2005. (IROS 2005)*., pp. 2505-2510, Alberta, 2005
- [70] D. Campolo, G. Cavallo, F. Keller, D. Accoto, P. Dario, E. Guglielmelli, Design and development of a miniaturized 2-axis force sensor for tremor analysis during locomotion in small-sized animal models, *27th Annual International Conference of the Engineering in Medicine and Biology Society, 2005. IEEE-EMBS 2005*, pp. 5054-5057, 2005
- [71] G. Cavallo, D. Campolo, E. Guglielmelli, S. Vollaro, F. Keller, Mechatronics and Phenomics: a case-study on tremor detection during locomotion in small-sized animals, *The 1st IEEE / RAS-EMBS International Conference on Biomedical Robotics and Biomechatronics.*, Pisa, 2006
- [72] S.H. Fatemi, *Reelin mutations in mouse and man: from reeler mouse to schizophrenia, mood disorders, autism and lissencephaly*, *Molecular Psychiatry*, Vol.6, N.2, pp 129-133, 2001
- [73] A.S.Fonseca, F.R.Pereira, R.Santos, Validation of a new computerized system for recording and analyzing drug-induced tremor in rats, *Journal of Pharmacological and Toxicological Methods*, 46, (137-143), 2002
- [74] S. Baron-Cohen, S. Wheelwright, A. Cox, G. Baird, T. Charman, J. Swettenham, A. Drew and P. Doehring, Early identification of autism by the Checklist for Autism in Toddlers (CHAT), *J.R. Soc. Med.* 93, 521-525 (2000)
- [75] C. Lord, S. Risi, L. Lambrecht Jr., E. H. Cook, B. L. Leventhal, P. C. DiLavore, A. Pickles and M. Rutter, The autism diagnostic observation schedule-generic: a standard measure of social and communication deficits associated with the spectrum of autism, *J. Autism Dev. Disord.* 30,205-223 (2000).



- [76] P. Teitelbaum, O. Teitelbaum, J. Nye, J. Fryman and R. G.Maurer, Movement analysis in infancy may be useful for early diagnosis of autism, Proc. Natl. Acad. Sci. USA 95, 13982-13987 (1998).
- [77] O. Teitelbaum, T. Benton, P. K. Shah, A. Prince, J. L. Kelly and P. Teitelbaum, Eshkol-Wachman movement notation in diagnosis: the early detection of Asperger's syndrome, Proc. Natl. Acad.Sci. USA 101, 11909-11914 (2004).
- [78] B. Kemp, A. J. M. W. Janssen, B. van der Kamp, Body position canbe monitored in 3D using miniature accelerometers and earth-magneticfield sensors, Electroencephalography and Clinical Neurophysiology,Vol. 109, pp. 484-488, 1998.
- [79] E. R. Bachmann, X. Yun, D. McKinney, R. B. McGhee, M. J. Zyda,Design and Implementation of MARG Sensors for 3-DOF OrientationMeasurement of Rigid Bodies, Proc. of the 2003 IEEE Intl. Conf. onRobotics and Automation (ICRA 2003), Taipei, Taiwan, September 14-19, 2003.
- [80] R. Zhu and Z. Y. Zhou, A Real-Time Articulated Human MotionTracking Using Tri-Axis Inertial/Magnetic Sensors Package, IEEETrans. on Neural Systems and Rehabilitation Engineering, Vol. 12, No.2, 2004.
- [81] D. Campolo, F. Keller and E. Guglielmelli, Inertial/magnetic sensors based orientation trackingon the group of rigid body rotations with application to wearable devices, in: Proc. IEEE/RSJInt. Conf. on Intelligent Robots and Systems, Beijing, pp. 4762-4767 (2006).
- [82] P. L. Rosin, Assessing Error of Fit Functions for Ellipses, GraphicalModels and Image Processing, Vol. 58, No. 5, pp. 494-502, 1996.
- [83] Blackburn M, van Vliet P, Mockett SP. Reliabilityof measurements obtained with the modified Ashworth scale in the lowerextremities of people with stroke. Phys Ther 2002;82:25-34.
- [84] Green J, Forster A, Young J. A test-retestreliability study of the Barthel Index, the Rivermead Mobility Index,the Nottingham Extended Activities of Daily Living Scale and the FrenchayActivities Index in stroke patients. Disabil Rehabil 2001;23:670-676.
- [85] van der Lee JH, Beckerman H, Lankhorst GJ, BouterLM. The responsiveness of the Action Research Arm test and the Fugl-MeyerAssessment scale in chronic stroke patients. J Rehabil Med 2001;33:110-113.

Giuseppe Cavallo

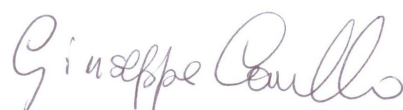
- [86] Lennon S, Johnson L. The modified Rivermead mobility index: validity and reliability. *Disabil Rehabil* 2000;22:833-839.
- [87] Reinstein L, Staas WE, Marquette CH. A rehabilitation evaluation system which complements the problem-oriented medical record. *Arch Phys Med Rehabil* 1975;56:396-398
- [88] Badley EM. An introduction to the concepts and classifications of the international classification of impairments, disabilities, and handicaps. *Dis Rehabil* 1993;15:161-178
- [89] Karni A, Meyer G, Jezard P, Adams MM, Turner R, Unterleider LG. Functional MRI evidence for adult motor cortex plasticity during motor skill learning. *Nature* 1995;377:155-158.
- [90] Crisostomo RA, Garcia MM, Tong DC. Detection of diffusion-weighted MRI abnormalities in patients with transient ischemic attack: correlation with clinical characteristics. *Stroke*. 2003;34:932-937.
- [91] Sanes, J. N., 2003. Neocortical mechanisms in motor learning. *Curr Opin Neurobiol* 13 (2), 225-231.
- [92] Muellbacher, W., Ziemann, U., Wissel, J., Dang, N., Kofler, M., Facchini, S., Boroojerdi, B., Poewe, W., Hallett, M., 2002. Early consolidation in human primary motor cortex. *Nature* 415 (6872), 640-644.
- [93] M. I. Jordan, and D. E. Rumelhart, Forward models: Supervised learning with a distal teacher. *Cognitive Science* 16:307-354 (1992)
- [94] Wolpert D.M., Z. Ghahramani, and M. I. Jordan, An internal model for sensorimotor integration. *Science* 269:1880-1882 (1995)
- [95] M. Kawato, Internal models for motor control and trajectory planning. *Curr. Opin. Neurobiol.* 9: 718-727 (1999)
- [96] Annett J. Motor imagery: perception or action? *Neuropsychologia* 1995;33(11):1395-417.
- [97] Bohan M, Pharmer JA, Stokes AF. When does imagery practice enhance performance on a motor task? *Percept. Mot. Skills* 1999;88(2):651-8.
- [98] M. L. Aisen, H. I. Krebs, N. Hogan, F. McDowell, and B. T. Volpe, The effect of robot assisted therapy and rehabilitative training on motor recovery following stroke. *Arch. Neurol.* 54:443-6 (1997)

Giuseppe Cavallo

- [99] D. J. Reinkensmeyer, N. Hogan, H. I. Krebs, S. L. Lehman, and P. S. Lum, Rehabilitators, robots, and guides: Newtools for neurological rehabilitation, in *Biomechanics and Neural Control of Posture and Movement*, J. Winters and P. Crago (Eds.), pp.516-533, Springer-Verlag (2000)
- [100] H. I. Krebs, N. Hogan, M. L. Aisen, and B.T. Volpe, Robot-aided neurorehabilitation. *IEEE Trans Rehabil Eng*6:75-87 (1998)
- [101] D. M. Wolpert, R. C. Miall, and M. Kawato, Internal models in the cerebellum. *Trends Cogn. Sci.* 2:338-347 (1998)
- [102] Jeannerod M. Mental imagery in the motor context. *Neuropsychologia* 1995;33(11):1419-32.
- [103] S. Clark, F. Tremblay, and D. Ste-Marie, Differential modulation of corticospinal excitability during observation, mental imagery and imitation of hand actions. *Neuropsychologia* 42(1):105-112(2004)
- [104] P. Dechent, K. D. Merboldt, and J. Frahm, Is the human primary motor cortex involved in motor imagery? *Brain Res Cogn Brain Res* 19(2):138-144 (2004)
- [105] H. H. Ehrsson, S. Geyer, and E. Naito, Imagery of voluntary movement of fingers, toes, and tongue activates corresponding body-part-specific motor representations. *J Neurophysiol.* 90(5):3304-3316,(2003)
- [106] P. L. Jackson, M. F. Lafleur, F. Malouin, C. L. Richards, and J. Doyon, Functional cerebral reorganization following motor sequence learning through mental practice with motor imagery. *Neuroimage*, 20(2):1171-1180 (2003)
- [107] S. H. Johnson-Frey, Stimulation through simulation? Motor imagery and functional reorganization in hemiplegic stroke patients. *Brain Cogn* 55(2):328-331 (2004)
- [108] J. M. Kilner, Y. Paulignan, and D. Boussaoud, Functional connectivity during real vs imagined visuomotor tasks: an EEG study. *Neuroreport* 15(4): 637-42 (2004)
- [109] G. Van Dijck, M. Van Hulle, J. Van Vaerenbergh, Hybrid feature subset selection for the quantitative assessment of skills of stroke patients in activity of daily living tasks, in *Proc. 28th IEEE EMBS Annual International Conference*, pp. 2474-2477, New York City, USA, 2006.

Giuseppe Cavallo

- [110] S. Lehericy, E. Gerardin , J. B. Poline, S. Meunier, P. F. Van de Moortele, D. Le Bihan, and M. Vidailhet, Motor execution and imagination networks in post-stroke dystonia. *Neuroreport* 15(12):1887-90 (2004)
- [111] D. M. Wolpert, Z. Ghahramani, and J. R. Flanagan, Perspectives and problems in motor learning. *Trends Cognitive Sciences* 5:487-94 (2001).
- [112] T. S. Buchanan, and D. A. Shreeve, An evaluation of optimization techniques for the prediction of muscle activation patterns during isometric tasks. *J. Biomech. Eng* 118(4):565-74 (1996)
- [113] J. P. Dewald, P. S. Pope, J. D. Given, T.S. Buchanan, and Rymer W. Z., Abnormal muscle coactivation patterns during isometric torque generation at the elbow and shoulder in hemiparetic subjects. *Brain* 118:495-510 (1995)
- [114] T. K. Koo, A. F. Mak, L. Hung, and J. P. Dewald, Joint position dependence of weakness during maximum isometric voluntary contractions in subjects with hemiparesis. *Arch. Phys. Med. Rehabil.* 84(9):1380-6 (2003)
- [115] T. J. Sejnowski, Making smooth moves. *Nature* 394:725-26 (1998)
- [116] B. Bobath, *Adult hemiplegia: evaluation and treatment*, London: William Heinemann Medical Books (1978)
- [117] S. Brunnstrom, *Movement therapy in hemiplegia: a neuro physiological approach*, New York: Harper and Row (1970)
- [118] J. Carr, and R. Shepard, *Neurological rehabilitation*, Oxford: Butterworth-Heinemann (1998)
- [119] C. Perfetti, *Der hemiplegische Patient. Kognitiv-therapeutische Ubungen*, Munchen: Richard Pflaum Verlag GmbH & Co (1997)
- [120] V. Mathiowetz, G. Kashman, G. Volland, K. Weber, M. Dowe, and S. Rogers, Grip and pinch strength: Normative data for adults. *Arch. Phys. Med. Rehabil.* 66:69-74 (1985)
- [121] S. G. Chung, E. Van Rey, E. J. Roth , and L.Q. Zhang, Aging-Related Changes in Achilles' Tendon Reflexes. *Arch. Phys. Med. Rehabil.* 84:E14 (2003)



- [122] J. Deutsch, J. Latonio, G. Burdea, and R.Boian, Post-Stroke Rehabilitation with the Rutgers Ankle System -A case study. *Presence* 10:416-430 (2001)
- [123] S. Le Bozec, S. Goutal, and S. Bouisset, Dynamic postural adjustments associated with the development of isometric forces in sitting subjects. *Life Sciences* 320:715-20 (1997)
- [124] S. M. Walsh, C. L. Saltzman, K. D. Talbot, R. L. Aper, and T. D. Brown, In vivo validation of in vitro testing of hallux flexor mechanics. *Clin Biomechanics* 11:328-2 (1996)
- [125] L. Peebles, and B. J. Norris, Adult data. The handbook of adult anthropometrical and strength measurements -Data for design safety, Department of Trade and Industry, London, UK (1998)
- [126] S. Pheasant, *Bodyspace. Anthropometry, ergonomics and the design of work*, pp. 84-85, Taylor & Francis, London, UK (1999)
- [127] G. Kurillo, M. Mihelj, M. Munih, and T. Bajd, Grasping and manipulation in virtual environment using 3 by 6 finger device, in *Proc. 9th IEEE International Conference on Rehabilitation Robotics*, pp. 131-134, Chicago, IL, USA, 2006.
- [128] Twitchell, TE. The restoration of motor function following hemiplegia in man. *Brain* 1951;74:443-80
- [129] Chen R, Cohen LG, Hallett M. Nervous system reorganization following injury. *Neuroscience* 2002;111:761-773
- [130] Morganti F, Gaggioli A, Castelnuovo G, Bulla D, Vettorello M, Riva G. The use of technology-supported mental imagery in neurological rehabilitation: a research protocol. *Cyberpsychol. Behav.* 2003;6(4):421-7.
- [131] Nair DG, Purcott KL, Fuchs A, Steinberg F, Kelso JA. Cortical and cerebellar activity of the human brain during imagined and executed unimanual and bimanual action sequences: a functional MRI study. *Brain Res. Cogn Brain Res.* 2003;15(3):250-60.
- [132] Naito E, Kochiyama T, Kitada R, Nakamura S, Matsumura M, Yonekura Y et al. Internally simulated movement sensations during motor imagery activate cortical motor areas and the cerebellum. *J. Neurosci.* 2002;22(9):3683-91.

Giuseppe Cavallo

- [133] S. Mazzoleni, J. Van Vaerenbergh, A. Toth, M. Munih, E. Guglielmelli, and P. Dario, ALLADIN: A novel mechatronic platform for assessing post-stroke functional recovery, in Proc. 9th IEEE International Conference on Rehabilitation Robotics (ICORR 2005), Chicago, IL, 2005, pp.156-159.
- [134] J. Van Vaerenbergh, S. Mazzoleni, A. Toth, E. Guglielmelli, M. Munih, E. Stokes, G. Fazekas, and S. De Ruijter, Assessment of recovery at stroke patients by whole-body isometric force-torque measurements, of functional tasks I: mechanical design of the device, in Proc. 3rd European Medical and Biological Engineering Conference (EMBEC 2005), Prague, Czech Republic, 2005, IFMBE Proc. 2005 11(1), ISSN: 1727-1983, paper 1834.
- [135] S. Mazzoleni, G. Cavallo, M. Munih, J. Cinkelj, M. Jurak, J. Van Vaerenbergh, D. Campolo, E. Guglielmelli, Towards application of a mechatronic platform for whole-body isometric force-torque measurements to functional assessment in neuro-rehabilitation, accepted to 2007 IEEE International Conference on Robotics and Automation (ICRA), Rome, Italy, 2007
- [136] B. Rohrer, S. Fasoli, H. I. Krebs, R. Hughes, B. Volpe, W. R. Frontera, J. Stein, and N. Hogan, Movement Smoothness Changes during Stroke Recovery, The Journal of Neuroscience, 2002, 22(18):8297-8304.
- [137] M. Jurak, and L. Kocsis, Algorithms for the automatic calculation of the gait reaction force parameters measured on instrumented treadmill, in Gepeszet 2004. Proc. 4th Conference on Mechanical Engineering, Budapest, Hungary, 2004, pp. 749-753.
- [138] W. Bowman, and A. Azzalini, Applied Smoothing Techniques for Data Analysis, Oxford University Press, 1997.
- [139] C. Orizio, R. Perini, B. Diemont, M. M. Figini, and A. Veicsteinas, Spectral analysis of muscular sound during isometric contraction of biceps brachii, J Appl Physiol, 1990.
- [140] M. T. Tarata, Mechanomyography versus Electromyography, in monitoring the muscular fatigue, BioMed Eng Online, 2003, 2:3.
- [141] Berthoz, A., Multisensory control of movement, Oxford: Oxford University Press, 1993.
- [142] E.V. Evarts, U. Shinoda, S. Wise, Neurophysiological Approaches to Higher Brain Functions, Wiley, 'New York-Freund, H. J., 1984.



- [143] S. Komblum, Requin J., Eds. Preparatory States and Processes, Erlbaum, Hillsdale, NJ, 1984.
- [144] A.P. Georgopoulos, J.T. Massey, Cognitive spatial-motor processes, Experimental Brain Research, vol 65, pp. 361-370, 1988.
- [145] F. Lacquaniti, C. Maioli, The Role of Preparation in Tuning Anticipatory and Reflex Responses during Catching, Journal of Neuroscience, vol. 9, pp. 134-148, 1989.
- [146] G.J.K. Alderson, D.J. Sully, H.G. Sully, An operational analysis of a one-handed catching task using high speed photography, J. Mot. Behav., vol 6, pp. 217-226, 1974.
- [147] R. H. Sharp, H. T. A. Whiting, Information-processing and eye movement behavior in a ball catching skill, J. Hum. Mov. Stud, vol 1, pp. 124-131, 1975.
- [148] D.N. Lee, Visuo-motor coordination in space-time, in Tutorials in Motor Behavior, Amsterdam: G. E. Stelmach -J. Requin, eds., pp. 281-295, 1980.
- [149] Y. Tanaka, T. Tsuji, M. Kaneko, Task readiness impedance in human arm movements for virtual ball-catching task, The 29th Annual Conference of the IEEE, vol. 1, pp. 478-483, 2003
- [150] F. Lacquaniti, C. Maioli, Adaptation to suppression of visual information during catching, Journal of Neuroscience, vol. 9, pp. 149-159, 1989.
- [151] F. Lacquaniti, C. Maioli, Anticipatory and reflex coactivation of antagonist muscles in catching, Brain Res., vol. 406, pp. 373-378, 1987.
- [152] N. Yang, M. Zhang, C. Huang, D. Jin, Synergic analysis of upper limb target-reaching movements, Journal of biomechanics, vol. 35, pp.739-746, 2002.
- [153] H. Gomi, M. Kawato, Human arm stiffness and equilibrium-point trajectory during multi-joint movement, Biol. Cybern., vol. 76, pp. 163-171, 1997.
- [154] T. Flash, N. Hogan, The coordination of arm movements: An experimentally confirmed mathematical model, The Journal of Neuroscience, vol. 5, pp. 1688-1703, 1985.

Giuseppe Cavallo

- [155] T. Tsuji , P. G. Morasso, K. Goto, K. Ito, Human hand impedance characteristics during maintained posture, *Biological Cybernetics* , vol. 72, pp. 475-485, 1995.
- [156] Y. Noguchi, T. Tsuji, K. Harada, M. Kaneko, Learning of Virtual Impedance Parameters in Non-contact Impedance Control using Neural Networks, *Journal of the Robotics Society of Japan*, vol. 18, pp. 561-568, 2000.
- [157] N. Hogan, The mechanics of multi-joint posture and movement control, *Biol. Cybern.*, vol. 52, pp. 315-331, 1985.
- [158] H. Gomi, M. Kawato, Equilibrium-point control hypothesis examined by measured arm stiffness during multi joint movement, *Science*, vol. 272, pp. 117-120, 1996.
- [159] N. Hogan, An organizing principle for a class of voluntary movements, *Journal of Neuroscience*, vol. 4, 1984.
- [160] C. Bonato, C. Miniussi, P.M. Rossini. Transcranial magnetic stimulation and cortical evoked potentials: a TMS/EEG co-registration study. *Clin Neurophysiol*; vol. 117, pp.1699-1707, 2006.
- [161] M. Zago, G. Bosco, V. Maffei, M. Iosa, Y. P. Ivanenko and F. Lacquaniti, Fast Adaptation of the Internal Model of Gravity for Manual Interceptions: Evidence for Event-Dependent Learning, *Journal of Neurophysiology*, 93:1055-1068, 2005.

Giuseppe Cavallo